博 士 論 文 (Abridged)

Studies on abiotic stress-responsive genes in pearl millet (*Pennisetum glaucum* (L.) R. Br.)

（トウジンビエの非生物的ストレス応答遺伝子に関する研究）

于　培

YU　PEI

Abstract

Abiotic stress negatively affects the yield of many crops. Pearl millet (*Pennisetum glaucum* (L.) R. Br., syn. *Cenchrus americanus* (L.) Morrone), is the sixth most economically important C4 cereal crop with the ability that can grow in marginal environments characterized by low and/or unstable rainfall, poor soil conditions and high temperature where other cereals such as rice, wheat, maize, and even sorghum are likely to fail to produce economic yields.

In this study, an important stress-related transcription factor family, *SQUAMOSA* promoter binding protein (SBP)-like transcription factor family was comprehensive analyzed. The SBPs represent a family of plant-specific transcription factors which play essential roles in plant growth, development, and stress responsiveness. In this study, 18 putative *SBP*s (*PgSBP*s) were identified in the genome of pearl millet on the basis of the SBP domain. One or two zinc finger-like structure(s) and a nuclear localization signal (NLS) were found in the SBP domains of all the PgSBPs. Fourteen *PgSBP*s were distributed on 7 chromosomes unevenly, while the other 4 were located on the scaffolds (i.e., non-chromosomal genomic sequences). Moreover, all the *PgSBP*s were clustered into seven groups (I-VII) based on the phylogenetic analysis. The intron/exon structures and the motif composition were similar between *PgSBP*s within the same groups. *PgSBP*s in groups V and VII were predicted as the targets of two microRNAs, *PgmiR156q* and *PgmiR529b*. Some *PgSBP*s have abscisic acid (ABA)-responsive elements and stress-responsive elements in their promoters. Expression levels of these *PgSBP*s were upregulated by abiotic stresses and downregulated by ABA. Together, this study shows a comprehensive overview of *PgSBP*s and provides vital information for elucidating the biological functions of *PgSBP*s.

Table of contents

Chapter 1

General introduction

1.1 Abiotic stresses

The world's population is increasing and already reached 7.7 billion in 2019 (United Nations Department of Economic and Social Affairs, and Population Division, 2019). In order to feed the increasing population, the production of agricultural food must be increased by 70 percent by 2050 (Tilman et al., 2011). Abiotic stresses, including drought, salinity, heat, and cold, will trigger various physiological, biochemical, and molecular responses that adversely affect many cellular processes in plants (Wang et al., 2003; Hasanuzzaman et al., 2013). The plant productivity will be limited ultimately, which causes crop losses in the world (Boyer, 1982; Qin et al., 2011; Bailey-Serres et al., 2012).

1.2 Abscisic acid (ABA)

1.2.1 ABA, a key plant stress-responsive hormone

Many physiological, biochemical, and molecular changes were induced and in turn, the entire metabolic processes were changed when plants were exposed to abiotic stresses (Wang et al., 2003). Plants synthesize various phytohormones, key regulators of plant growth and development and the essential mediators of environmental stress responses, to combat the effect of stress-induced injuries (Seki et al., 2002; Shinozaki and Yamaguchi-Shinozaki, 2007; Sreenivasulu et al., 2012). Among various phytohormones, ABA is the key regulator of abiotic stress tolerance in plants (Wani, 2015; Finkelstein, 2013).

1.2.2 Roles of ABA in plants

ABA has multiple functions in growth and development of plants under stress and non-stress conditions. The level of ABA is significantly increased under stress conditions, such as drought and salinity, stimulating stomatal closure, alter in gene expression, and adaptive physiological responses (Seki et al., 2002; Finkelstein, 2013; Kim et al., 2010; Cutler et al., 2010; Shinozaki and Yamaguchi-Shinozaki, 2007; Yamaguchi-Shinozaki and Shinozaki, 2006). ABA also plays important roles in many cellular processes including seed development, dormancy, germination, vegetative growth, and modulation of root architecture (Finkelstein et al., 2008; Harris, 2015; Xiong and Yang, 2003).

1.3 SQUAMOSA promoter binding protein (SBP) transcription factor family

In higher plants, transcription factors (TFs) play vital roles in the regulating physiological processes and adapting to environmental stresses through various signal transduction pathways (Chen and Rajewsky, 2007). *SQUAMOSA* promoter binding protein (SBP) and SBP-like protein (SPL) genes encode a plant-specific family of TFs, which have a highly conserved SBP domain with approximately 76 amino acid residues. This conserved domain consists of two zinc-finger structures (Zn-1 and Zn-2) and a nuclear localization signal (NLS) (Yamasaki et al., 2004). Two *SBP* genes were first identified in *Antirrhinum majus* with the ability for binding the promoter region of the floral meristem identity gene *SQUAMOSA* (Klein et al., 1996). *SBP* genes also play important roles in the regulation of plant architecture (Jiao et al., 2010), the vegetative phase change (Wang et al. 2009), anthocyanin biosynthesis (Gou et al., 2011), gibberellin (GA) biosynthesis and signaling (Yu et al., 2012), and stress responses (Cui et al., 2014).

1.4 MicroRNAs

MicroRNAs, non-coding 20–24 nucleotides small RNAs, induce either transcript cleavage or transcription repression (Chen, 2009). Many *SBP* genes are targeted by a

microRNA, *miR156*. In Arabidopsis, this *miR156*/*SBP* module regulates root development (Cui et al., 2014) and affects secondary metabolite accumulation, which can improve stress tolerance (Yu et al., 2015). In rice, *OsSPL14*, which is regulated by *OsmiR156*, improves panicle branching, grain yield, and shoot branching (Jiao et al. 2010; Miura et al., 2010). In switchgrass, the overexpression of *miR156* induces aerial bud formation, while the overexpression of *SPL4* suppresses bud formation and tillering (Gou et al., 2017). In alfalfa, *miR156* improves drought and heat stress tolerance by silencing *SPL13* (Arshad et al., 2017; Matthews et al., 2019). Another microRNA, *miR529*, sharing 14–16 nucleotides with *miR156*, was also reported to target *SBP*s in plants (Zhang and Ling, 2018).

1.5 Pearl millet

1.5.1 The importance of pearl millet

Pearl millet (*Pennisetum glaucum* (L.) R. Br., syn. *Cenchrus americanus* (L.) Morrone), belonging to family Poaceae and subfamily Panicoideae, is a highly cross-pollinated diploid (2n = 2x = 14) with a draft genome size of 1.79 Gb (Varshney et al., 2017).

Pearl millet is the sixth most economically important C4 cereal crop with nutrient-rich seeds to provide food security for almost 90 million people inhabiting across the high temperature regions of Africa and Asia (Shivhare and Lata, 2017). It has the ability that can grow in marginal environments characterized by low and/or unstable rainfall, poor soil conditions and high temperature where other cereals such as rice, wheat, maize, and even sorghum are likely to fail to produce economic yields (Vadez et al., 2012). It is cultivated on approximately 31 million ha of land and contributes around 50% of total global millet production. Pearl millet grains are high in nutrient composition, with 8-19% protein, low starch, high fiber (1.2 g/100 g) (Nambiar et al., 2011), and are considered as an inexpensive source of energy compared to staple cereals such as wheat, rice, and maize in terms of micronutrients (Zinc and Iron) (Kumar et al., 2016a).

1.5.2 Research progress of functional stress-related genes in pearl millet

Pearl millet has excellent nutrient composition and exceptional buffering capacity against variable climatic conditions and pathogen attack, which is anticipated to be equipped with better tolerance mechanisms than other cereals to combat different abiotic stresses. There were thousands of differential expression genes (DEGs) were found in pearl millet under drought and salinity stress conditions based on transcriptome analysis (Dudhate et al., 2018; Shinde et al., 2018), but limited studies were conducted to explore the functions of stress-related genes in pearl millet.

Shinde *et al*. (2019) characterized one pearl millet gene, *PgNAC21* (Shinde et al., 2019). The results showed that its expression was induced by salinity stress and ABA, and Arabidopsis plants overexpressing *PgNAC21* exhibited better seed germination, heavier fresh weight, greater root length and higher expression levels of some stress-related genes including *GLUTATHIONE S-TRANSFERASE* (*GSTF6*), *COLD-REGULATED 47* (*COR47*) and *RESPONSIVE TO DEHYDRATION 20* (RD20)) under salinity stress. One pearl millet gene from the ABA STRESS RIPENING (ASR) family, *PgASR3*, was reported to confer multiple abiotic stress tolerance in its transgenic Arabidopsis with higher growth rate (shoot and root length), relative water content (RWC), chlorophyll and proline as compared to wildtype (WT) plants (Meena et al., 2020). A pearl millet Na^+/H^+ antiporter was isolated and characterized by Rajagopal et al., 2007, whose expression level was significantly induced by salinity stress and ABA and confers to salinity stress tolerance in transgenic yeas and *Brassica juncea* (Rajagopal et al., 2007). Constitutive overexpression of a stress-inducible small GTP-binding protein PgRab7 from pearl millet enhanced abiotic stress tolerance with increased alkaline phosphatase (ALP) activities in transgenic tobacco (Agarwal et al., 2008). Recombinant PgHsc70 (Pearl millet cytoplasmic Hsp70) protein purified from *E. coli* possessed in vitro chaperone activity and protected *PgHsc70* expressing bacteria from damage caused by heat and salinity stress (Reddy et al., 2010).

1.6 Objective

Although the roles of SBP genes have been revealed in many plants, such as Arabidopsis (Cardon et al., 1999), rice (Xie et al., 2006), cotton (Zhang et al., 2014), foxtail millet (Bennetzen et al., 2012), pepper (Zhang et al., 2016), tobacco (Han et al., 2016) and sorghum (Chang et al., 2016), their functions in pearl millet are unclear. In order to characterize the SBP genes in pearl millet (*PgSBP*s), we analyzed the SBP genes in the pearl millet genome and performed phylogenetic analysis, conserved domain analysis, and the *cis*-element analysis for these genes. Expression patterns of *PgSBP*s, *PgmiR156*, and *PgmiR529* under various conditions were also investigated. The results can help to perform further functional analysis of *PgSBP*s in pearl millet.

Chapter 2

Materials and methods

2.1 Plant materials

One inbred pearl millet line, ICMB 843, which had been evaluated as a drought-tolerant line in the International Crop Research Institute of Semi-Arid Tropics (ICRISAT), India, was used in this study. Seeds were sown in the soil that consists of akadama, vermiculite, charcoal, slow-release, and quick-release fertilizers. Plants were grown in a greenhouse in Tokyo, Japan, under the sunlight in July and August (with the day length of 13.5-14.5 hours and the maximum light intensity ~1300 $\mu mol \cdot m^{-2} \cdot s^{-1}$). The temperature and relative humidity in the greenhouse were set for 25°C and 65%, respectively. These settings kept the actual temperature 25-28°C and the actual humidity 55-75%. For gene cloning, root samples were collected from 4-week-old plants, while for expression analysis, roots and leaves were collected from 4-week-old untreated plants (Control) and plants treated with 15% (w/v) PEG6000, 250 mM NaCl, 42℃ and 25 μM abscisic acid (ABA) for 6 h and 24 h.

2.2 Identification and bioinformatic analysis of PgSBPs

In a previous study, the whole genome of pearl millet was sequenced, and individual gene and protein sequences were deduced from this whole genome sequence (Varshney et al., 2017). These protein sequences were submitted as the query to the HMMER hmmscan program to identify *ab initio* the proteins with an SBP domain (Pfam accession number: PF03110). CD-search (https://www.ncbi.nlm.nih.gov/Structure/cdd/wrpsb.cgi) and Pfam (https://pfam.xfam.org/family/PF03110) were used to confirm the presence of the SBP domain in those proteins. Sequence logos for the SBP domain were generated by WebLogo 2.8.2 (http://weblogo.berkeley.edu/logo.cgi) (Crooks et al., 2004). The molecular weight (MW) and theoretical isoelectric point (pI) of PgSBPs were

calculated using the ProtParam tool on the ExPASy server (https://web.expasy.org/protparam/). The conserved motifs were obtained by MEME 5.0.5 program (http://meme-suite.org/tools/meme) with the following parameters: a maximum number of motifs 16; motif width range 6–50 residues (Bailey et al., 2009). Intron/exon structures of *PgSBP*s were determined by aligning the cDNA sequences of *PgSBP*s to their corresponding genomic sequences using Gene Structure Display Server 2.0 (http://gsds.cbi.pku.edu.cn/index.php) (Hu et al., 2015). The *cis*-acting elements in the 2000 bp promoter regions were detected by the online website PlantCARE (http://bioinformatics.psb.ugent.be/webtools/plantcare/html/) (Lescot, 2002).

2.3 Chromosome location, the percentage identity matrix, and phylogenetic analysis

Chromosome locations of the *PgSBP*s were determined by the Map Gene 2 Chromosome v2 (http://mg2c.iask.in/mg2c_v2.0/). A percentage identity matrix of PgSBP was built on the basis of the sequence alignment using Clustal Omega (https://www.ebi.ac.uk/Tools/msa/clustalo/) and presented as a heatmap in HemI 1.0 (Deng et al., 2014). The SBP domain sequences of pearl millet, sorghum, rice, and foxtail millet were used together for the phylogenetic analysis. Multiple sequence alignment was conducted by ClustalW with default parameters in the MEGA X software. The phylogenetic tree was reconstructed by using the maximum-likelihood (ML) method with 1000 bootstrap replications based on the JTT+G model (Kumar et al., 2016b). The resulting tree was visualized using iTOL v4 (Letunic and Bork, 2019).

2.4 Prediction of *PgSBP*s targeted by *PgmiRNA*s

The 290 microRNA sequences of pearl millet were obtained from previous small RNA sequencing data (Shinde et al., 2020). *PgSBP*s targeted by *PgmiR156q* or *PgmiR529b* were predicted by the psRNATarget server a(http://plantgrn.noble.org/psRNATarget/) with default parameters (Dai et al., 2018a).

2.5 DNA isolation and PCR amplification

Genomic DNA was extracted from the root of 4-week-old pearl millet plants with a DNeasy Plant Mini Kit (QIAGEN, Germany) in accordance with the manufacturer's instructions. *PgSBP* sequences were obtained by PCR using the genomic DNA as the template. Primers used for the PCR are listed in Table 2.1. The PCR products were gel-purified by FastGene Gel/PCR Extraction Kit (Genetics, Japan) and sequenced by Macrogen, Japan.

Table 2.1. Primers used for amplifying unknown parts of *PgSBP*s

Gene	Primer sequence (5'-3')
PgSBP1	FW: GTAACGTGGATAAGAAGGTGAAATGTCC
	RV: CTGGTTACCAAATTACCCATGGATTTC
PgSBP2	FW: GCAACCTCTACGACAGCGGCTTCGACC
	RV: CCTTGGCGTGGAACTCGCAGACCTTG
PgSBP3	FW: CTGCTCTGGGACTGGGGCGACAACG
	RV: GGCAGCGGAGGTTCCATCCGCTGTCAGAG
PgSBP5 Part1	FW: CTCGCTTCCCATCAACCTTCATC
	RV: CAGGCAGTGCTGCATTTGGGCTAGGAAGG
PgSBP5 Part2	FW: CAAGTCCTGATAACTGTGTGCGTATTC
	RV: CACCATTAGACTCCATAAATCACGAAG
PgSBP5 Part3	FW: CTAGCTGTCTGAAGAACTGAATGTTAC
	RV: CATCTCTAGATGCCATTTTGTATCTGC
PgSBP6	FW: CCTTCCATTTATTTCCTTGACTTCTCC
	RV: GAGATCTATCGATGATGTACAATTCGC
PgSBP8	FW: GGTAGGCTGAACGTGACCACGTCCTC
	RV: CCTTGGCGTGGTACTCGCAGACCTTG
PgSBP13	FW: ATGGACCGCAAGGACAAGTCCCGCAGG
	RV: ACCGGCTGCATTGCTGGCAGAAGCGCTG
PgSBP17	FW: CTTTTTACTCCTTCCGTCTACCAGTACC
	RV: ATTCTACGAATGGGCACAGTAGCA
PgSBP18	FW: TCCACGGCCTCAAGTTCGGCAAGAAG
	RV: TCCACGGCCTCAAGTTCGGCAAGAAG

2.6 RNA extraction and quantitative reverse transcription-PCR (qRT-PCR) analysis

Total RNA was extracted from leaves and roots of the 4-week-old pearl millet plants with a NucleoSpin RNA Plant kit (MACHEREY-NAGEL, Germany) according to the manufacturer's instructions. cDNA was synthesized from 1 μg of the total RNA with Prime Script Reverse Transcriptase (Takara, Japan) and the oligo (dT) primer. The expression levels of *PgSBP*s were quantified by the quantitative reverse transcription-PCR (qRT-PCR), which was performed with the StepOne Real-Time PCR System (Applied Biosystems, USA) and the TB Green Premix Ex Taq™ (Takara, Japan). The PCR cycle was: 95 °C for 30 s, followed by 40 cycles at 95 °C for 5 s and 60 °C for 30 s, and then a dissociation curve analysis was performed at 95 °C for 60 s, 55 °C for 30 s, and 95 °C for 30 s. The *Ubiquitin* (*UBQ*) gene (GenBank accession number XM_004977046.2) (Anup et al., 2017) was used as the reference gene. Gene-specific primers for the *PgSBP*s were designed by the Primer-BLAST online server (https://www.ncbi.nlm.nih.gov/tools/primer-blast/) based on the MIQE guidelines (http://rdml.org/miqe). The primers are listed in Supplementary Table 2.2. The comparative Ct method was used to quantify expression levels (Schmittgen and Livak, 2008). For microRNA expression analysis, the cDNA was reverse-transcribed from 2 μg of the total RNA with the Mir-XTM miRNA First-Strand Synthesis Kit (Takara, Japan). For the qRT-PCR, the entire sequences of mature microRNAs were used for forward primers, and the mRQ3' primer from the kit was used as the reverse primer. U6 snRNA from the kit was used as the reference RNA. The PCR was conducted as described above.

Table 2.2. Primers for qRT-PCR

Gene	Forward (5'-3')	Reverse (5'-3')	PCR product (bp)
PgSBP1	GTCCAACAGGACGCATCTCA	GGGCGAATGTAACCCTCCAA	127
PgSBP2	GCAGCAGGTTTCATGTGCTC	GTAGTGTCCGCTCTCTTGGG	148
PgSBP3	CACTGGTGCCAGCGAGAACA	CGAACCAGCTGAGGCTGAGG	111
PgSBP4	ACTCAGCTGCACCCTGGCCT	CTGCTGCAATGGCGCTGCTC	160
PgSBP5	TCTCTCTTCTGTCATCGGCCA	AGGAGAAGAACTGCCACGC	138
PgSBP6	TCCCGCCAAGAGGGGGCTAC	TGCTCGCAGACCTTGTGGCG	118
PgSBP7	GGAGGACGAGCATCCGCAGC	GGGCAACGACGAGGAGGTGC	142
PgSBP8	CCACCACCAGCAGGAGCAGC	GCACACCGACGAGCACGACA	106
PgSBP9	CAGATGGTTCGTGGGGTTCA	TGCATGACGGAGTTGGAGAC	115
PgSBP10	CTGGACTTCGAGCTGCCCGC	GGCGCCGGTTGTGTCCATCA	147
PgSBP11	CGGCGGGCACAACAAGGACA	CCCTGCTGCTGCACTCGGAC	122
PgSBP12	CCGGTGGTGGCGACAAGGAC	AGCACGACGAGGGCCTTGGA	143
PgSBP13	ATGCAGCCGGTTCCACGAGC	CGTGTCCGCCGAGCTCTTCC	106
PgSBP14	CGCAGGAAGCCGCAACCAGA	GCCTTGGAGCCGGGAACGAC	109
PgSBP15	CTGCAGACGTAGGCTCGCCG	GCAGGCGCGCGATGACAGTA	152
PgSBP16	GCGCGCAGAGCAGCCATTTG	GACGGCGAGCTGTTCGACCC	175
PgSBP17	GTACCAGCCACAACCGGCCC	GACCCGTAGCCCAGGAGCCA	120
PgSBP18	CGGAGCTCCCTTCGGGTGGA	GAGGGTGCCACAGGGTTGGC	166

Chapter 3

Results

3.1 Identification, molecular cloning, and gene feature analysis of *PgSBP*s

Eighteen SBP genes (*PgSBP1-18*) were identified in the pearl millet genome and their sequences were deposited in the NCBI database (Table 3.1). The lengths of these genomic sequences varied from 2082 bp (*PgSBP10*) to 12237 bp (*PgSBP1*). The coding sequences of *PgSBP*s ranged from 501 bp (*PgSBP13*) to 2964 bp (*PgSBP15*), with the deduced proteins ranging from 166 to 987 amino acids in length and from 10.67 (PgSBP16) to 94.01 (PgSBP1) kDa in protein mass. The predicted pI of the PgSBPs varied from 5.54 (PgSBP16) to 10.28 (PgSBP14). Among all the PgSBPs, 12 members are basic proteins with pI values more than 7.0 and the rest are acidic proteins (Table 3.1). PgSBPs in general have low identities to each other, except that PgSBP7 and PgSBP13 share 66% identity, PgSBP7 and PgSBP14 share 62% identity, and PgSBP13 and PgSBP17 share 62% identity (Figure 3.1 and Table 3.2). Fourteen *PgSBP*s (*PgSBP1-14*) were unevenly distributed on 7 chromosomes with one gene on Chr1 and Chr4; two on Chr3, Chr5, and Chr6; and three on Chr2 and Chr7 (Figure 3.2). *PgSBP15*, *PgSBP16*, *PgSBP17,* and *PgSBP18* were found to be located on scaffolds (i.e., genomic sequences that have not been assigned to any chromosome) 2013, 2474, 2484, and 4011, respectively.

Table 3.1. The 18 *PgSBP*s identified in pearl millet and their sequence characteristics.

Name	Gene ID	Gene length (bp)	CDS length (bp)	No. of amino acids (aa)	MW	pI
PgSBP1	MW561430	12237	2568	855	94.01	5.59
PgSBP2	MW561431	2966	1314	437	45.84	6.75
PgSBP3	MW561432	2994	858	285	31.10	9.72
PgSBP4	MW561433	3467	1482	493	52.46	9.14
PgSBP5	MW561434	2546	1164	387	39.23	9.58
PgSBP6	MW561435	3153	1191	396	43.16	7.47
PgSBP7	MW561436	4390	858	285	30.30	8.33
PgSBP8	MW561437	2463	1296	431	45.84	9.24
PgSBP9	MW561438	3027	1302	433	47.42	8.95
PgSBP10	MW561439	2082	846	281	29.98	9.34
PgSBP11	MW561440	4262	2424	807	90.07	6.78
PgSBP12	MW561441	2995	540	179	19.03	10.19
PgSBP13	MW561442	2947	501	166	17.41	9.98
PgSBP14	MW561443	3625	774	257	27.73	10.28
PgSBP15	MW561444	4231	2964	987	10.89	5.96
PgSBP16	MW561445	5312	2934	977	10.67	5.54
PgSBP17	MW561446	2670	864	287	30.41	8.95
PgSBP18	MW561447	3245	966	322	34.01	6.56

Table 3.2. The percentage identity matrix of PgSBP proteins.

Proteins	PgSBP1	PgSBP2	PgSBP3	PgSBP4	PgSBP5	PgSBP6	PgSBP7	PgSBP8	PgSBP9	PgSBP10	PgSBP11	PgSBP12	PgSBP13	PgSBP14	PgSBP15	PgSBP16	PgSBP17	PgSBP18
PgSBP1	1.00	0.26	0.20	0.22	0.28	0.24	0.26	0.29	0.24	0.24	0.23	0.31	0.28	0.21	0.25	0.24	0.25	0.19
PgSBP2	0.26	1.00	0.24	0.27	0.29	0.38	0.33	0.48	0.28	0.25	0.25	0.39	0.40	0.21	0.31	0.31	0.31	0.22
PgSBP3	0.20	0.24	1.00	0.35	0.23	0.21	0.25	0.20	0.34	0.21	0.25	0.27	0.33	0.23	0.23	0.20	0.30	0.26
PgSBP4	0.22	0.27	0.35	1.00	0.27	0.28	0.25	0.27	0.55	0.22	0.30	0.36	0.37	0.19	0.29	0.28	0.34	0.25
PgSBP5	0.28	0.29	0.23	0.27	1.00	0.32	0.33	0.34	0.27	0.26	0.27	0.42	0.42	0.22	0.31	0.31	0.37	0.24
PgSBP6	0.24	0.38	0.21	0.28	0.32	1.00	0.33	0.34	0.29	0.21	0.26	0.42	0.45	0.22	0.32	0.29	0.27	0.19
PgSBP7	0.26	0.33	0.25	0.25	0.33	0.33	1.00	0.31	0.31	0.34	0.37	0.52	0.66	0.62	0.28	0.28	0.32	0.29
PgSBP8	0.29	0.48	0.20	0.27	0.34	0.34	0.31	1.00	0.25	0.26	0.31	0.38	0.44	0.23	0.29	0.31	0.29	0.24
PgSBP9	0.24	0.28	0.34	0.55	0.27	0.29	0.31	0.25	1.00	0.23	0.30	0.35	0.38	0.23	0.28	0.28	0.31	0.26
PgSBP10	0.24	0.25	0.21	0.22	0.26	0.21	0.34	0.26	0.23	1.00	0.24	0.35	0.39	0.36	0.23	0.25	0.25	0.21
PgSBP11	0.23	0.25	0.25	0.30	0.27	0.26	0.37	0.31	0.30	0.24	1.00	0.36	0.36	0.29	0.34	0.42	0.32	0.19
PgSBP12	0.31	0.39	0.27	0.36	0.42	0.42	0.52	0.38	0.35	0.35	0.36	1.00	0.66	0.30	0.43	0.43	0.49	0.26
PgSBP13	0.28	0.40	0.33	0.37	0.42	0.45	0.66	0.44	0.38	0.39	0.36	0.66	1.00	0.35	0.50	0.40	0.62	0.28
PgSBP14	0.21	0.21	0.23	0.19	0.22	0.22	0.62	0.23	0.23	0.36	0.29	0.30	0.35	1.00	0.23	0.24	0.29	0.27
PgSBP15	0.25	0.31	0.23	0.29	0.31	0.32	0.28	0.29	0.28	0.23	0.34	0.43	0.50	0.23	1.00	0.33	0.27	0.20
PgSBP16	0.24	0.31	0.20	0.28	0.31	0.29	0.28	0.31	0.28	0.25	0.42	0.43	0.40	0.24	0.33	1.00	0.29	0.19
PgSBP17	0.25	0.31	0.30	0.34	0.37	0.27	0.32	0.29	0.31	0.25	0.32	0.49	0.62	0.29	0.27	0.29	1.00	0.55
PgSBP18	0.19	0.22	0.26	0.25	0.24	0.19	0.29	0.24	0.26	0.21	0.19	0.26	0.28	0.27	0.20	0.19	0.55	1.00

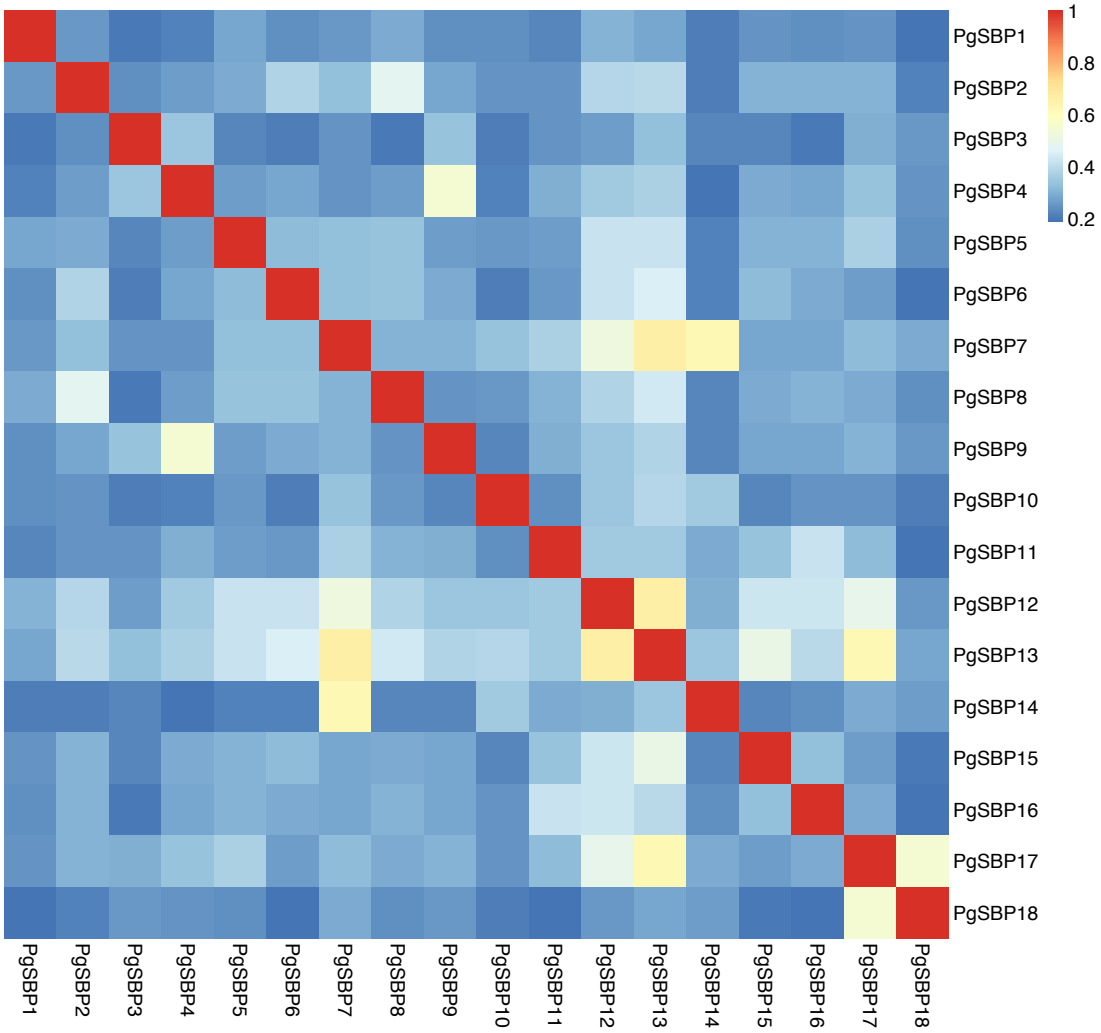

Figure 3.1. The percentage identity matrix of PgSBP proteins. The heatmap was conducted based on the PgSBP protein sequences. The colored bar indicates the correlation of protein sequences of two genes, blue represents a low correlation, red represents a high correlation. The correlated values of the PgSBP proteins are listed in Table 3.2.

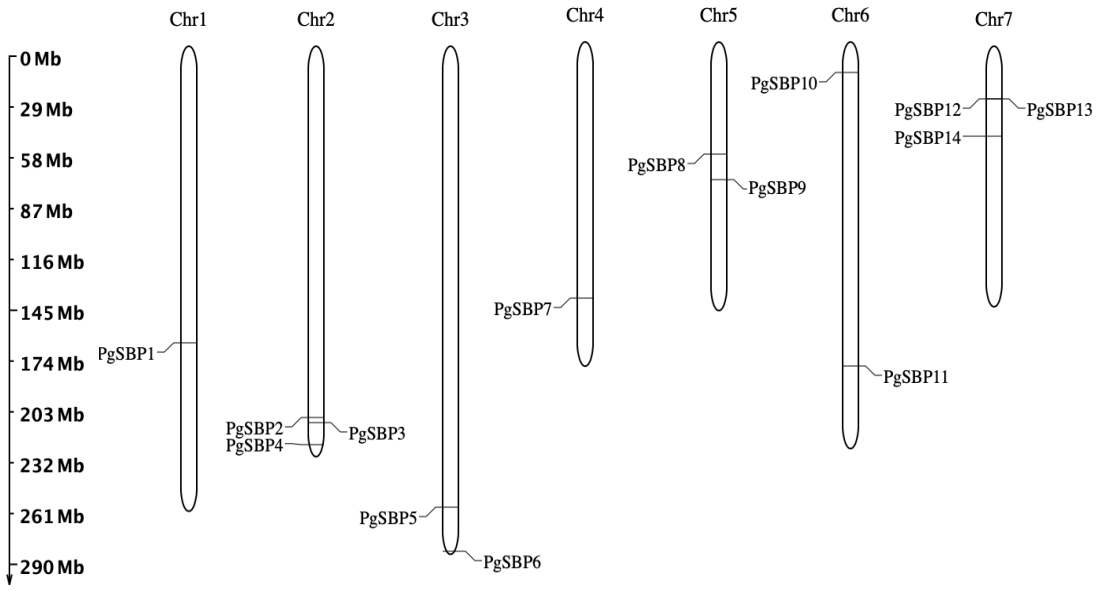

Figure 3.2. Positions of SBP genes in pearl millet chromosomes. The chromosome number is indicated at the top of each bar (i.e., chromosome). The scale is represented in mega base (Mb).

3.2 Sequence alignments and phylogenetic analysis of SBP domains

SBP domains have high similarity with each other and most of the PgSBPs have both Zn-1 and Zn-2 as well as an NLS in their SBP domains (Figure 3.3). However, PgSBP7, PgSBP10, PgSBP14, and PgSBP18 lack Zn-1 and a part of Zn-2 (Figure 3.3A). PgSBP11, PgSBP15, and PgSBP16 contain not only a SBP domain but also an ankyrin (ANK) domain (Figure 3.4), which is associated with protein-protein interactions (Michaely and Bennett, 1992).

A phylogenetic tree was constructed using the highly conserved SBP-domains of the 18 PgSBPs, 27 *Setaria italica* SBP proteins (SiSBPs), 39 *Sorghum bicolor* SBP proteins (SbSBPs), and 19 *Oryza sativa* SBP proteins (OsSBPs). The resulting tree suggests that the 18 PgSBPs can be classified into seven groups (group I to VII, Figure 3.5) and that all of these groups contain at least one SBP member from each species. Group VII is the largest group with six PgSBPs included. Groups I and II are the smallest groups with only one PgSBP member included.

Table 3.3. The SBP domain sequences selected for phylogenetic analysis.

Protein	Protein sequence of SBP-domain
PgSBP1	CQVPGCEVDIRELKGYHRRHRVCLRCAHASAVMLDGVQKRYCQQCGKFHVLLDFDEDKRSCRRKLERHNKRRRR
PgSBP2	CQAEACKADLSAAKHYHRRHKVCEFHAKAAAVVAAGKQQRFCQQCSRFHVLAEFDEAKRSCRKRLTEHNRRRRK
PgSBP3	CQAERCNADLSDAATYNRRHKVCQTHSKAPVVLVAGLRQRFCQQCSRFHELSEFDETRRSCRLRLAGHNERRRK
PgSBP4	CQVEGCKIDLSSAKDYHRKHKVCEAHSKAPKVVVAGLERRFCQQCSRFHGLDVFDQKKRSCRRRLNDHNARRRK
PgSBP5	CQVEGCKIDLSSAKDYHRKHKVCEAHSKAPKVVVAGLERRFCQQCSRFHGLDVFDQKKRSCRRRLNDHNARRRK
PgSBP6	CQAEGCKADLSSAKRYHRRHKVCEHHSKAPVVVTAGGLHQRFCQQCSRFHLLDEFDDAKKSCRKRLADHNRRRRK
PgSBP7	MRFCQQCSRFHLLAEFDDTKRSCRKRLDGHNRRRRK
PgSBP8	CQAEGCKADLSGAKHYHRRHKVCEYHAKASVVAAGGKQQRFCQQCSRFHVLTEFDEAKRSCRKRLAEHNRRRRK
PgSBP9	CQVEGCNVDLSSAKAYHRKHKVCEDHAKAPKVVVAGLERRFCQQCSRFHGLAEFDQNKRSCRRRLTHHNARRRK
PgSBP10	FHSLGEFDDTKRSCRKRLDGHNRRRRK
PgSBP11	CQVDGCHADLSGSRDYHKRHKVCEAHTRTSVVCIKNVEHRFCQQCSRFHLLQEFDEGKKSCRSRLSKHNVRRRK
PgSBP12	CQVERCAADLHGARRYYRRHKVCEVHSKALVVLVAGLRQRFCQQCSRFHDLLEFDDSKHSCRRRLAGHNERRRK
PgSBP13	CQAERCNADLSDAATYNRRHKVCQTHSKAPVVLVAGLRQRFCQQCSRFHELSEFDETRRSCRLRLAGHNERRRK
PgSBP14	RFHLLAEFDDAKRSCRKRLDGHNRRRRK
PgSBP15	CQVDDCRADLTSAKDYHRRHKVCETHSKTTKAVVASQMQRFCQQCSRFHPLAEFDEGKRSCRRRLAGHNRRRRK
PgSBP16	CQVEGCGADLTAAKDYHRRHKVCEMHAKASTAVVGNTVQRFCQQCSRFHLLQEFDEGKRSCRRRLAGHNRRRRK
PgSBP17	MHTKTPRVVVAGIEQRFCQQCSRFHELSEFDQGKRSCRRRLIGHNERRRK
PgSBP18	FHQLHEFDQQKRSCRRRLTGHNERRRR
SiSBP1	CQAEGCKADLSAAKHYHRRHKVCEFHAKAAAVAAAGKQQRFCQQCSRFHVLAEFDEAKRSCRKRLTEHNRRRRK
SiSBP2	CQVEGCGLELGTAKEYHRKHRVCEAHTKCPRVVVAGQERRFCQQCSRFHALSEFDQKKRSCRRRLSDHNARRRK
SiSBP3	CQVEGCKIDLSSAKDYHRKHKVCEAHSKAPKVVVAGLERRFCQQCSRFHGLDVFDQKKRSCRRRLNDHNARRRK

SiSBP4	CQVEGCKIDLSSAKDYHRKHKVCEAHSKAPKVVVAGLERRFCQQCSRFHGLDVFDQKKRSCRRRLNDHNARRRK
SiSBP5	CQVEGCKIDLSSAKDYHRKHKVCEAHSKAPKVVVAGLERRFCQQCSRFHGLDVFDQKKRSCRRRLNDHNARRRK
SiSBP6	CQVEGCKIDLSSAKDYHRKHKVCEAHSKAPKVVVAGLERRFCQQCSRFHGLDVFDQKKRSCRRRLNDHNARRRK
SiSBP7	CQVEGCGVDLSGAKPYHCRHKVCSMHTKTPRVVVAGIEQRFCQQCSRFHELPEFDQGKRSCRRRLIGHNERRRK
SiSBP8	CAVDGCKADLSKCRDYHRRHKVCEAHSKTPVVVVSGREMRFCQQCSRFHLLAEFDDAKRSCRKRLDGHNRRRRK
SiSBP9	CQAERCNADLSDAATYNRRHKVCQTHSKAPVVLVAGLRQRFCQQCSRFHELSEFDETRRSCRLRLAGHNERRRK
SiSBP10	CQVERCAADLHDARRYYRRHKVCETHSKALVVLIAGLRQRFCQQCSRFHELLEFDDNKHSCRRRLAGHNERRRK
SiSBP11	CQAEGCKADLSSAKRYHRRHKVCEHHSKAPVVVTAGGLHQRFCQQCSRFHLLDEFDDAKKSCRKRLADHNRRRRK
SiSBP12	CQVPGCEADIRELKGYHRRHRVCLRCAHASAVILDGVQKRYCQQCGKFHVLLDFDEDKRSCRRKLERHNKRRRRK
SiSBP13	CQAEGCKADLSGAKHYHRRHKVCEYHAKASVVAAGGKQQRFCQQCSRFHVLTEFDEAKRSCRKRLAEHNRRRRK
SiSBP14	CQVEGCKVDLSSAKAYHRKHKVCEDHAKAPKVVVAGLERRFCQQCSRFHGLAEFDQNKRSCRRRLTHHNARRRK
SiSBP15	CQVDGCHADLSGARDYHKRHKVCEAHTRTSVVCIKNVEHRFCQQCSRFHLLQEFDEGKKSCRSRLAKHNGRRRK
SiSBP16	CQVDGCHADLSGARDYHKRHKVCEAHTRTSVVCIKNVEHRFCQQCSRFHLLQEFDEGKKSCRSRLAKHNGRRRK
SiSBP17	CQVDGCHADLSGARDYHKRHKVCEAHTRTSVVCIKNVEHRFCQQCSRFHLLQEFDEGKKSCRSRLAKHNGRRRK
SiSBP18	CQVDGCHADLSGARDYHKRHKVCEAHTRTSVVCIKNVEHRFCQQCSRFHLLQEFDEGKKSCRSRLAKHNGRRRK
SiSBP19	CSVEGCAADLSKGRDYHRRHKVCEAHSKTPVVTVAGQQQRFCQQCSRFHSLGEFDDTKRSCRKRLDGHNRRRRK
SiSBP20	CQVEGCNVDLTGAKTYHCRHKVCAMHAKAPLVVVNGIEQRFCQQCSRFHQLHEFDQQKRSCRRRLTGHNERRRR
SiSBP21	CQVEGCNVDLTGAKTYHCRHKVCAMHAKAPLVVVNGIEQRFCQQCSRFHQLHEFDQQKRSCRRRLTGHNERRRR
SiSBP22	CQVDDCRADLTSAKDYHRRHKVCETHSKTTKALVASQMQRFCQQCSRFHPLAEFDEGKRSCRRRLAGHNRRRRK
SiSBP23	CAVEGCTADLSKCRDYHRRHKVCEAHSKTPVVVVAGREMRFCQQCSRFHLLAEFDDTKRSCRKRLDGHNRRRRK
SiSBP24	CQVEGCHMELAGAKEYHRRHKVCEAHSKAPRVVVLGAEQRFCQQCSRFHAISEFDDAKRSCRRRLAGHNERRRK
SiSBP25	CSVDGCRSDLSRCREYHRRHRVCEAHSKTPVVVVGGQEQRFCQQCSRFHMLSEFDEGKKSCRKRLDGHNRRRRK
SiSBP26	CSVDGCRSDLSRCREYHRRHRVCEAHSKTPVVVVGGQEQRFCQQCSRFHMLSEFDEGKKSCRKRLDGHNRRRRK
SiSBP27	CQVEGCGADLTAAKDYHRRHKVCEMHAKASTAVVGNTVQRFCQQCSRFHLLQEFDEGKRSCRRRLAGHNRRRRK
SbSBP1	CQVEGCGADLTAAKDYHRRHKVCEMHAKASTAVVGNTVQRFCQQCSRFHLLQEFDEGKRSCRRRLAGHNRRRRK

SbSBP2 CQVDGCGVDLSAVKQYYCRHKVCYMHSKEPRVVVAGIEQRFCQQCSRFHQLPEFDQGKRSCRRRLIGHNERRRK
SbSBP3 CAVDGCKADLSKCRDYHRRHKVCEAHSKTPVVVVAGREMRFCQQCSRFHLLAEFDEAKRSCRKRLDGHNRRRRK
SbSBP4 CAVDGCKADLSKCRDYHRRHKVCEAHSKTPVVVVAGREMRFCQQCSRFHLLAEFDEAKRSCRKRLDGHNRRRRK
SbSBP5 CQAERCNANLMTDEKPYNRRHKVCEAHSKAPVVLVAGLRQRFCQQCSRFHELSEFDDIKRSCRLRLAGHNERRRK
SbSBP6 CQVERCNADMGVEKRYNRRHKVCDAHRKASVVLLAGLRQRFCQQCSRFHELSHFDDTKRSCRLRLAGHNERRRR
SbSBP7 CQVERCNADMGVEKRYNRRHKVCDAHRKASVVLLAGLRQRFCQQCSR
SbSBP8 CQVDGCHADLSGARDYHKRHKVCEAHTRTTVVCIKNVEHRFCQQCSRFHLLQEFDEGKKSCRSRLAKHNGRRRK
SbSBP9 CQVDGCHADLSGARDYHKRHKVCEAHTRTTVVCIKNVEHRFCQQCSRFHLLQEFDEGKKSCRSRLAKHNGRRRK
SbSBP10 CSVQGCDADLSRCRDYHRRHKVCEAHSKTPVVTVAGQQQRFCQQCSRFHLLGEFDEVKRSCRKRLDGHNRRRRK
SbSBP11 CQVEGCKVDLSSAKEYHRKHKVCEPHSKASKVVVAGLERRFCQQCSRFHGLSEFDQKKKSCRRRLNDHNARRRK
SbSBP12 CQVEGCKVDLSSAKEYHRKHKVCEPHSKASKVVVAGLERRFCQQCSRFHGLSEFDQKKKSCRRRLNDHNARRRK
SbSBP13 CQVEGCKVDLSSAKEYHRKHKVCEPHSKASKVVVAGLERRFCQQCSRFHGLSEFDQKKKSCRRRLNDHNARRRK
SbSBP14 CQVEGCKVDLSSAKEYHRKHKVCEPHSKASKVVVAGLERRFCQQCSRFHGLSEFDQKKKSCRRRLNDHNARRRK
SbSBP15 CQVEGCKVDLSSAKEYHRKHKVCEPHSKASKVVVAGLERRFCQQCSRFHGLSEFDQKKKSCRRRLNDHNARRRK
SbSBP16 CQVEGCKVDLSSAKEYHRKHKVCEPHSKASKVVVAGLERRFCQQCSRFHGLSEFDQKKKSCRRRLNDHNARRRK
SbSBP17 CQVEGCKVDLSSAKEYHRKHKVCEPHSKASKVVVAGLERRFCQQCSRFHGLSEFDQKKKSCRRRLNDHNARRRK
SbSBP18 CQVEGCKVDLSSAKEYHRKHKVCEPHSKASKVVVAGLERRFCQQCSRFHGLSEFDQKKKSCRRRLNDHNARRRK
SbSBP19 CQVEGCGLDLTRVKDYHRKHRVCEAHTKSPRVIVAGQERRFCQQCSRFHALSEFDQKKRSCRRRLSDHNARRRK
SbSBP20 CQAEGCKADLSAAKHYHRRHKVCEYHAKAGSVAAAGKQQRFCQQCSRFHVLAEFDEAKRSCRKRLTEHNRRRRK
SbSBP21 CSVDGCRSDLSRCREYHRRHKVCEAHSKTPVVVVAGQEQRFCQQCSRFHMLSEFDEGKRSCRKRLDGHNRRRRK
SbSBP22 CSVDGCRSDLSRCREYHRRHKVCEAHSKTPVVVVAGQEQRFCQQCSRFHMLSEFDEGKRSCRKRLDGHNRRRRK
SbSBP23 CSVDGCRSDLSRCREYHRRHKVCEAHSKTPVVVVAGQEQRFCQQCSRFHMLSEFDEGKRSCRKRLDGHNRRRRK
SbSBP24 CQVEGCHVALADAKDYHRRHKVCEAHSKAPRVVVLGAEQRFCQQCSRFHAISEFDEAKRSCRRRLAGHNERRRK
SbSBP25 CQAEGCKADLSSAKRYHRRHKVCEHHSKAPVVVTAGGLHQRFCQQCSRFHLLDEFDDAKKSCRKRLADHNRRRRK
SbSBP26 CAVEGCKADLSKCRDYHRRHKVCEAHSKTPVVVVAGREMRFCQQCSRFHLLAEFDADKRSCRKRLDGHNRRRRK

SbSBP27 CQVDDCRADLTSAKDYHRRHKVCETHSKTTKAVVANQAQRFCQQCSRFHPLAEFDEGKRSCRRRLAGHNRRRRK
SbSBP28 CQVDDCRADLTSAKDYHRRHKVCETHSKTTKAVVANQAQRFCQQCSRFHPLAEFDEGKRSCRRRLAGHNRRRRK
SbSBP29 CQVDGCNVDLTDVKPYYCRHKVCKMHSKEPRVVVNGLEQRFCQQCSRFHQLPEFDQLKKSCRRRLAGHNE
SbSBP30 CQVDGCNVDLTDVKPYYCRHKVCKMHSKEPRVVVNGLEQRFCQQCSRFHQLPEFDQLKKSCRRRLAGHNE
SbSBP31 CQVPGCEADIRELKGYHRRHRVCLRCAHAAAVMLDGVQKRYCQQCGKFHILLDFDEDKRSCRRKLERHNKRRRRK
SbSBP32 CQVPGCEADIRELKGYHRRHRVCLRCAHAAAVMLDGVQKRYCQQCGKFHILLDFDEDKRSCRRKLERHNKRRRRK
SbSBP33 CQAEGCKADLSGAKHYHRRHKVCEYHAKASVVAAGGKQQRFCQQCSRFHVLSEFDEVKRSCRKRLAEHNRRRRK
SbSBP34 CQVEGCKVDLSSAKDYNRKHKVCVAHSKAPKVVVAGLERRFCQQCSRFHGLAEFDQNKRSCRRRLTHHNARRRK
SbSBP35 CQVEGCKVDLSSAKDYNRKHKVCVAHSKAPKVVVAGLERRFCQQCSRFHGLAEFDQNKRSCRRRLTHHNARRRK
SbSBP36 CQVEGCKVDLSSAKDYNRKHKVCVAHSKAPKVVVAGLERRFCQQCSRFHGLAEFDQNKRSCRRRLTHHNARRRK
SbSBP37 CQVEGCKVDLSSAKDYNRKHKVCVAHSKAPKVVVAGLERRFCQQCSRFHGLAEFDQNKRSCRRRLTHHNARRRK
SbSBP38 CQVEGCKVDLSSAKDYNRKHKVCVAHSKAPKVVVAGLERRFCQQCSRFHGLAEFDQNKRSCRRRLTHHNARRRK
SbSBP39 CQVEGCKVDLSSAKDYNRKHKVCVAHSKAPKVVVAGLERRFCQQCSRFHGLAEFDQNKRSCRRRLTHHNARRRK
OsSBP1 CQVDGCTVNLSSARDYNKRHKVCEVHTKSGVVRIKNVEHRFCQQCSRFHFLQEFDEGKKSCRSRLAQHNRRRRK
OsSBP2 CSVEGCAADLSKCRDYHRRHKVCEAHSKTAVVTVAGQQQRFCQQCSRFHLLGEFDEEKRSCRKRLDGHNKRRRK
OsSBP3 CQVEGCNVDLSSAKPYHRKHRVCEPHSKTLKVIVAGLERRFCQQCSRFHGLAEFDQKKRSCRRRLHDHNARRRK
OsSBP4 CQVEGCGVELVGVKDYHRKHRVCEAHSKFPRVVVAGQERRFCQQCSRFHALSEFDQKKRSCRRRLYDHNARRRK
OsSBP5 CQAEGCKADLSAAKHYHRRHKVCDFHAKAAAVLAAGKQQRFCQQCSRFHVLAEFDEAKRSCRKRLTEHNRRRRK
OsSBP6 CQVEGCTADLTGVRDYHRRHKVCEMHAKATTAVVGNTVQRFCQQCSRFHPLQEFDEGKRSCRRRLAGHNRRRRK
OsSBP7 CQVEGCDITLQGVKEYHRRHKVCEVHAKAPRVVVHGTEQRFCQQCSRFHVLAEFDDAKKSCRRRLAGHNERRRR
OsSBP8 CQAEGCKADLSSAKRYHRRHKVCEHHSKAPVVVTAGLHQRFCQQCSRFHLLDEFDDAKKSCRKRLADHNRRRRK
OsSBP9 CQVPGCEADIRELKGYHRRHRVCLRCAHAAAVMLDGVQKRYCQQCGKFHILLDFDEDKRSCRRKLERHNRRRRK
OsSBP10 CQAEGCKADLSGAKHYHRRHKVCEYHAKASVVAASGKQQRFCQQCSRFHVLTEFDEAKRSCRKRLAEHNRRRRK
OsSBP11 CQVEGCGLELGGYKEYYRKHRVCEPHTKCLRVVVAGQDRRFCQQCSRFHAPSEFDQEKRSCRRRLSDHNARRRK
OsSBP12 CQVEGCKVDLSSAREYHRKHKVCEAHSKAPKVIVSGLERRFCQQCSRFHGLAEFDQKKKSCRRRLSDHNARRRK

OsSBP13	CQVERCGVDLSEAGRYNRRHKVCQTHSKEPVVLVAGLRQRFCQQCSRFHELTEFDDAKRSCRRRLAGHNERRRK
OsSBP14	CQVEGCGADLSGIKNYYCRHKVCFMHSKAPRVVVAGLEQRFCQQCSRFHLLPEFDQGKRSCRRRLAGHNERRRR
OsSBP15	CQVDDCRADLTNAKDYHRRHKVCEIHGKTTKALVGNQMQRFCQQCSRFHPLSEFDEGKRSCRRRLAGHNRRRRK
OsSBP16	CAVDGCKEDLSKCRDYHRRHKVCEAHSKTPLVVVSGREMRFCQQCSRFHLLQEFDEAKRSCRKRLDGHNRRRRK
OsSBP17	CQVEGCGVDLSGVKPYYCRHKVCYMHAKEPIVVVAGLEQRFCQQCSRFHQLPEFDQEKKSCRRRLAGHNERRRK
OsSBP18	CAVDGCKADLSKHRDYHRRHKVCEPHSKTPVVVVSGREMRFCQQCSRFHLLGEFDEAKRSCRKRLDGHNRRRRK
OsSBP19	CSVDGCRSDLSRCRDYHRRHKVCEAHAKTPVVVVAGQEQRFCQQCSRFHNLAEFDDGKKSCRKRLDGHNRRRRK

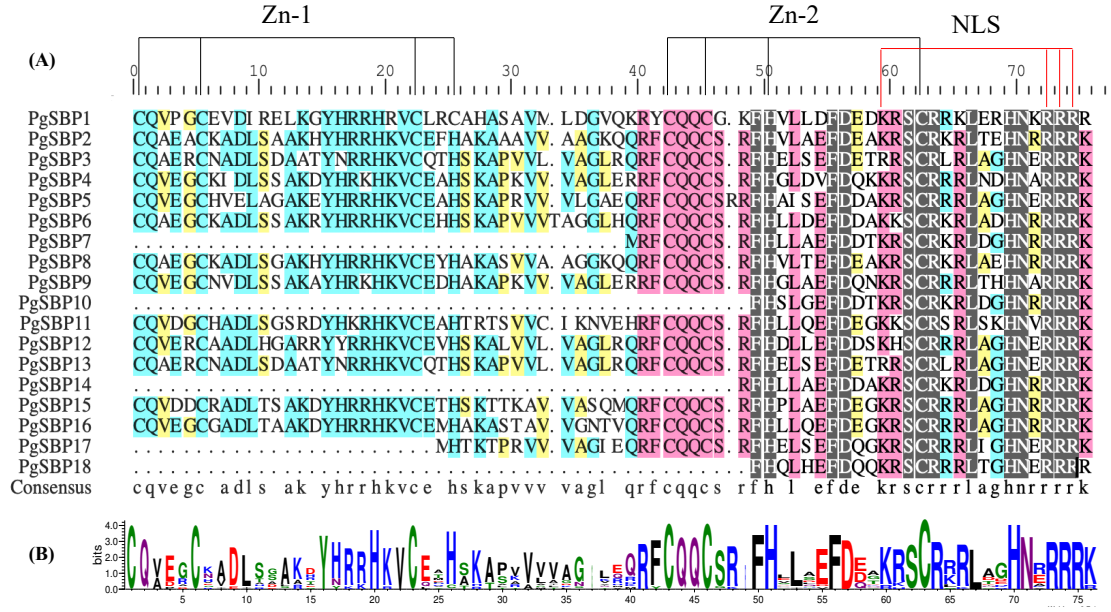

Figure 3.3. Alignment of PgSBPs. (A) Multiple alignment of SBP domains of PgSBPs obtained with DNAMAN software. The two conserved zinc-finger structures (Zn-1 and Zn-2) and NLSs are indicated. (B) Sequence logos for the SBP domain of PgSBPs. The overall height of each stack represents the extent of conservation at each position, while the height of the letters within each stack indicates the relative frequency of the corresponding amino acid.

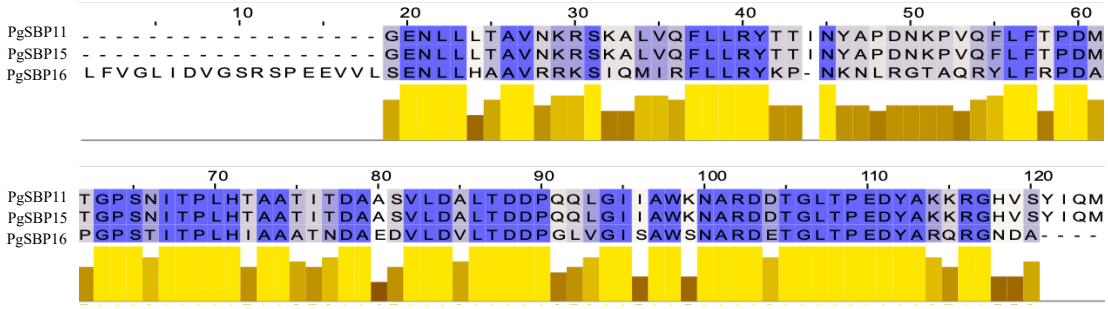

Figure 3.4. Alignment of ANK domain in PgSBP11, PgSBP15 and PgSBP16.

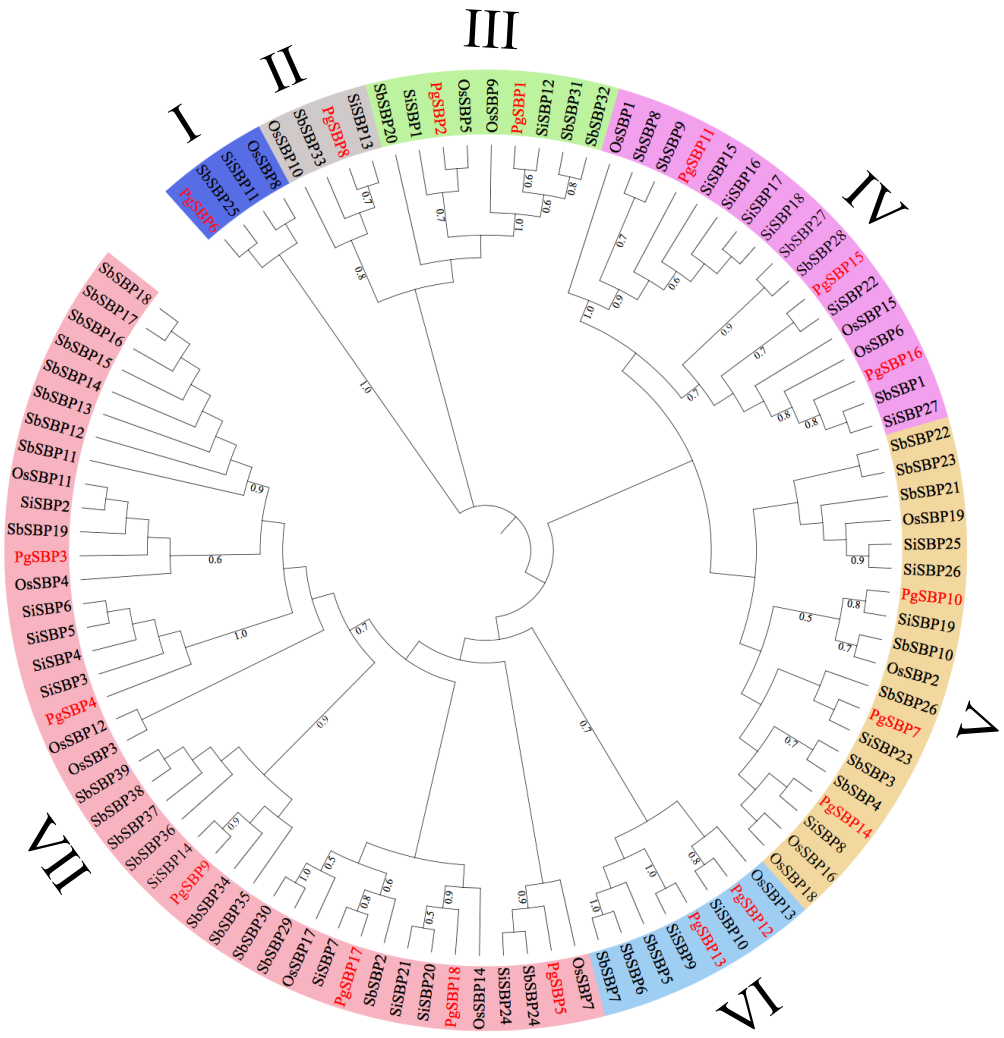

Figure 3.5. The maximum likelihood (ML) phylogenetic tree of SBP proteins from pearl millet (PgSBP), sorghum (SbSBP), foxtail millet (SiSBP) and rice (OsSBP). The SBP domain sequences, accession numbers/locus IDs, and data sources of all genes used for phylogenetic tree construction are listed in Supplementary Table 3.3.

3.3 Structural organization and conserved motif analysis of PgSBPs

Intron/exon structures of the 18 *PgSBP*s were analyzed by their genomic sequences and protein-coding sequences. The number of exons among *PgSBP*s ranged from 2 (*PgSBP12* and *PgSBP13*) to 11 (*PgSBP16*). The *PgSBP*s in the same group in the phylogenetic tree shared a similar intron/exon structure (Figure 3.6).

In addition to the SBP and ANK domains, 16 motifs were identified for the 18 PgSBPs (Figure 3.7, Table 3.4). The number of these motifs in each PgSBPs varies from 1 (PgSBP3) to 10 (PgSBP11 and PgSBP16) and the proteins in group IV possess the largest numbers of conserved motifs. Motif 1, motif 2, and motif 3 represent the N terminal, C terminal, and middle parts of the SBP domain, respectively. Some of these motifs are specific to some groups. These data support the idea that the PgSBPs in the same group have similar functions.

Table 3.4. Consensus sequences of 16 motifs identified in PgSBPs

Motif	Length (aa)	Consensus sequence
1	32	R**FH**L**L**AE**FD**DTKR**SCR**KR**L**DG**HN**R**RRR**KPQPD
2	39	PPR**CQ**AEG**C**KAD**L**SSAKR**Y**HRR**HKVC**EHHSKAPVVVTAG
3	8	Q**R**F**CQQC**S
4	50	R**T**DK**I**V**FKL**FGKE**P**KDF**P**VD**LR**EQ**I**LN**WL**SHC**P**TDM**E**S**YIRPGC**VI**L**TVY
5	48	VL**DA****LTDDP**QQL**G**IIA**W**KNAR**D**DT**G**LT**PE**D**YA**KK**R**GHVS**Y**IQM**V**QD**K**I
6	48	**K**M**FSDG**L**T**R**VLDSDCALSLLS**A**P**ANSS**GI**DVSRMV**R**PTEH**V**PMAQPLV**
7	29	**F**NMW**RF**RN**L**GI**F**AMERE**WC**AVVKM**LL**DFL
8	21	**MGSFGM**N**W**V**QK**N**S**MV**WDCENL**
9	10	**L**KL**G**KRAYFE
10	47	YPNSRP**R**TFLY**RP**AMLTVMGV**A**V**VCVCV**GILLHTFPRV**Y**AAPT**F**R**W**E
11	17	**R**D**QI**LH**FL**N**EL****GWL**FQ**R**
12	26	**EPGRFRSFLLDF**T**YPRVPSS**M**RD**G**WP**
13	49	WM**W**D**EL**DDHPAPWIEK**L**INM**S**NGG**FW**RT**G**WVYSRVQEC**L**TLSCN**G**SLM**L**
14	31	**MFYD**GR**QQTSL**L**F**G**Q**APYG**Q**M**RS**C**A**SSSWDN**
15	33	**GTRFS**P**F**A**APR**LDAN**W**P**GVIK**T**E**ENPF**YS**HHQ**I
16	9	**WDLNDW**R**WD**

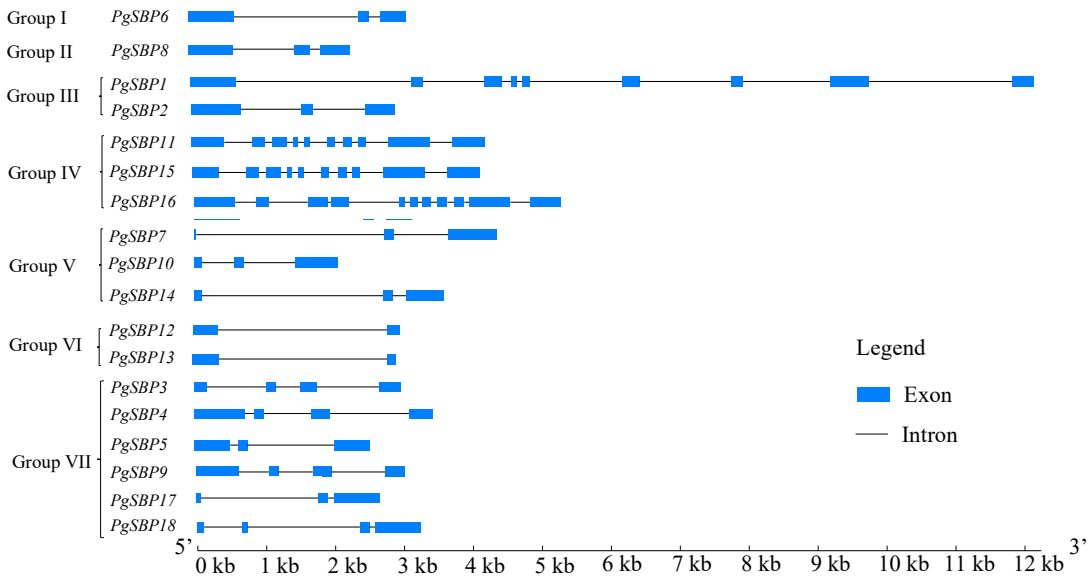

Figure 3.6. Exon/intron structures of *PgSBP*s. Exons and introns are indicated by blue rectangles and black horizontal lines, respectively.

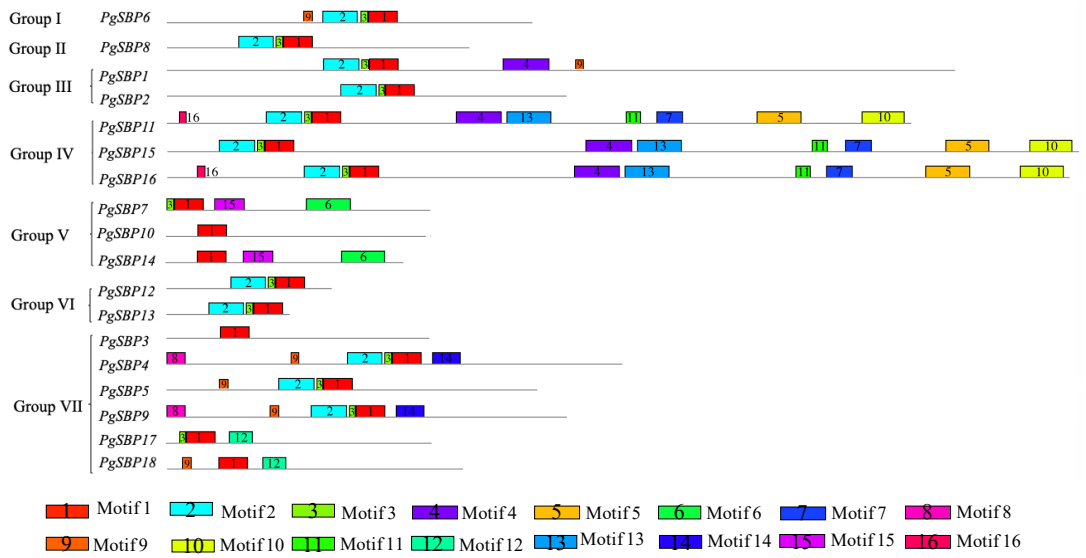

Figure 3.7. Distribution of conversed motifs in PgSBPs. Motifs indicated by boxes were detected by MEME and the number in boxes (1 to 16) represents motif 1 to motif 16, respectively. Box sizes indicate the length of the motifs and the consensus sequences of these motifs are presented in Table 3.4.

3.4 *Cis*-elements analysis in the promoter regions of *PgSBP*s

The *cis*-elements in the 2000-bp promoter regions of *PgSBP*s were identified and were categorized into six groups based on the predicted functions shown in Figure 3.8. The *cis*-elements identified include the elements regulating hormone responsiveness, such as the ABA-responsive elements (ABREs), the methyl jasmonate (MeJA)-responsive elements (CGTCA-motifs), auxin-responsive elements (TGA-elements and AuxRR-core elements), salicylic acid (SA)-responsive elements (TCA-element and SARE) and GA-responsive elements (GARE motifs, P-boxes, and TATC-boxes). Stress-associated *cis*-elements were also identified, such as the low-temperature responsive elements (LTREs), the drought-responsive elements (DREs), the MYB binding sites (MBSs), and TC-rich repeats. All the *PgSBP*s except *PgSBP3* and *PgSBP18* have some of those *cis*-elements, raising the possibility that most of the *PgSBP*s are either induced or repressed by phytohormones and/or abiotic stresses.

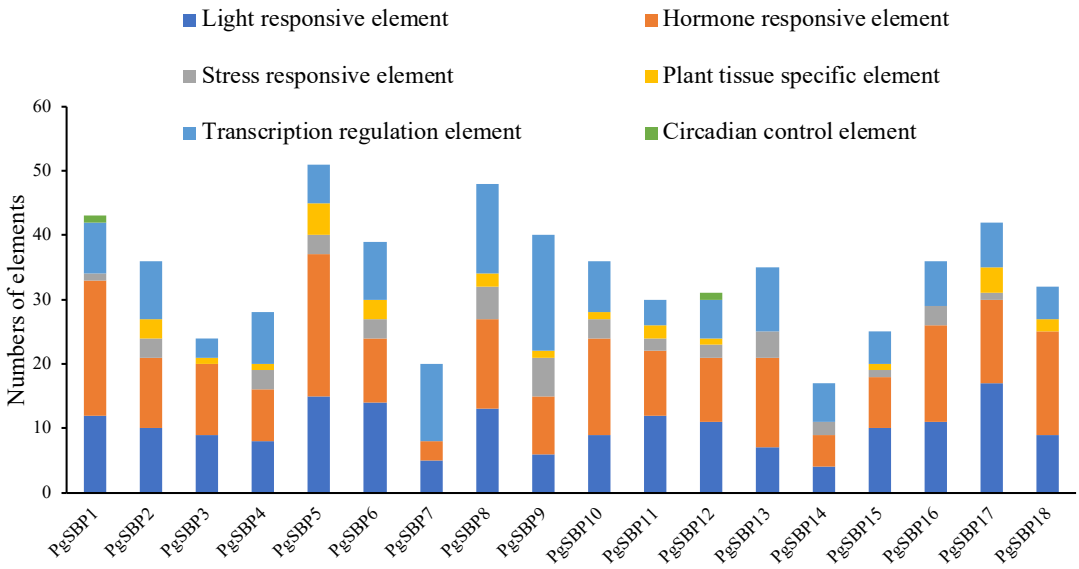

Figure 3.8. *Cis*-elements in promoter regions of *PgSBP*s. The elements were identified from 2000 bp upstream promoter regions.

3.5 The regulation of the *PgSBP*s transcript by *PgmiR156q* and *PgmiR529b*

Nine out of the 18 *PgSBP*s (*PgSBP3*, *PgSBP4*, *PgSBP5*, *PgSBP7*, *PgSBP9*, *PgSBP10*, *PgSBP14*, *PgSBP17*, and *PgSBP18*), which encode PgSBPs in the groups V and VII, were found to be potential targets of a pearl millet *miR156*, *PgmiR156q* (Figure 3.9A). All these genes, except *PgSBP4*, are also potential targets of a pearl millet *miR529*, *PgmiR529b* (Figure 3.10). The distances between their SBP domain-coding sequences and putative microRNA binding sites were similar between these *PgSBP*s (326 bp–418 bp) (Figure 3.9B). These results raise the possibility that these microRNA target sites originated from the common ancestor.

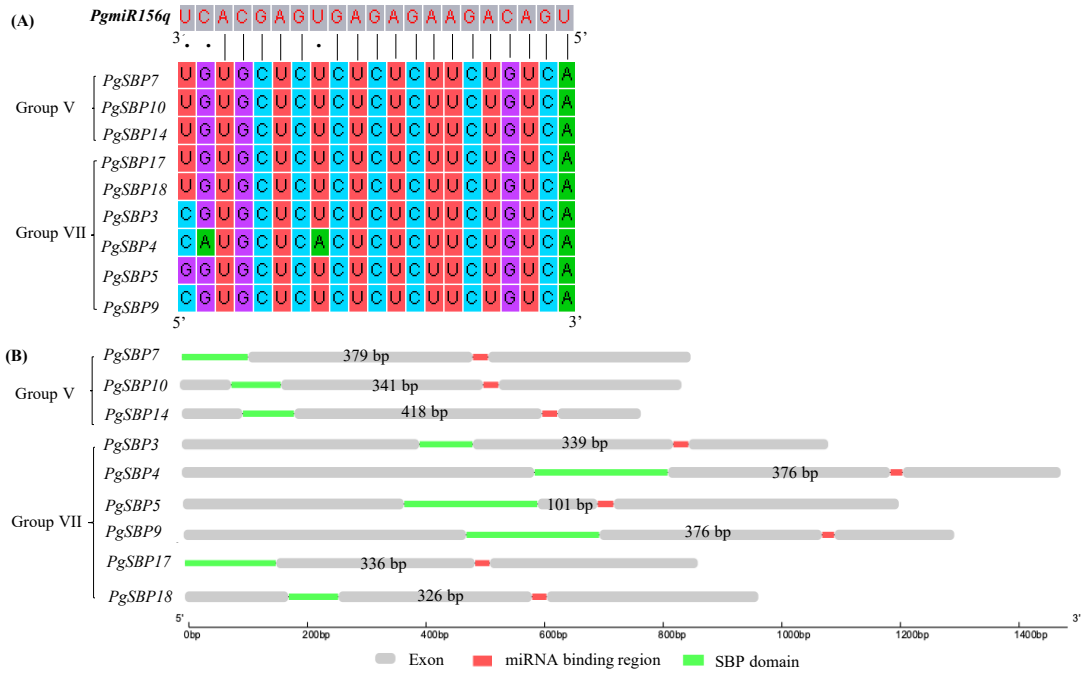

Figure 3.9. *PgSBP*s targeted by *PgmiR156q*. (A) Alignment of the *PgmiR156q* mature sequence with complementary sequences of *PgSBP*s. The dots between miRNAs and targeted *PgSBP* sequences indicate mismatches. (B) The positions of miRNA binding regions and SBP domains in the sequences of *PgSBP*s.

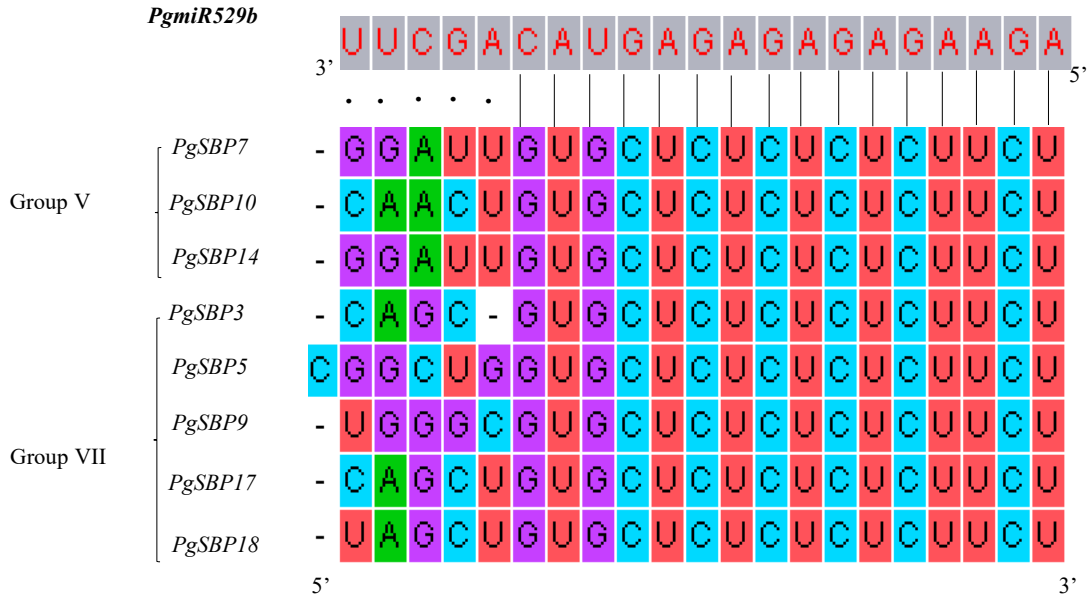

Figure 3.10. Sequence alignment of *PgmiR529* mature sequences with complementary sequences of *PgSBP*s. The dots between miRNAs and targeted *PgSBP* sequences indicate mismatches.

3.6 Expression profiles of *PgSBP*s, *PgmiR156q*, and *PgmiR529b* in different tissues under various abiotic stresses

In order to explore the possible functions of *PgSBP*s, the expression profiles of all *PgSBP*s were investigated in root and leaf tissues under salinity-stressed, drought-stressed, heat-stressed, and ABA-supplemented conditions with qRT-PCR (Figure 3.11). In leaf tissues, two genes, *PgSBP8* and *PgSBP10*, were upregulated by salinity stress and *PgSBP2* was upregulated by drought stress. Twelve out of 18 *PgSBP*s were upregulated by heat stress. In roots, most of the *PgSBP*s were upregulated by salinity, drought, and heat stresses. According to previous RNA sequencing data (Dudhate et al., 2018), the absolute expression levels of *PgSBP3*, *PgSBP10*, *PgSBP11*, *PgSBP15*, and *PgSBP16* were higher than the other *PgSBP*s in root tissues under a control condition (Figure 3.12). All these 5 *PgSBP*s were significantly induced by salinity, drought, and heat stresses (Figure 3.11). The expression of *PgSBP2* in roots was 205 and 119 times stronger in the presence of salinity and drought stresses, respectively, compared to expression in control roots. The expression of *PgSBP7* and *PgSBP13* in roots was also 109 times stronger in the presence of salinity stress than in control roots (Figure 3.11). Thus, although the absolute expression levels of these genes in roots are low (Figure 3.12), they may regulate salinity and/or drought stress responsiveness. Further studies are necessary to clarify their functions.

Expression of pearl millet *miR156* and *miR529* (*PgmiR156q* and *PgmiR529b*) was also examined under the same conditions. In general, the expression patterns of *PgmiR156q* and *PgmiR529b* were similar to each other and opposite to *PgSBP*s (Figure 3.11). For instance, *PgmiR156q* and *PgmiR529b* were downregulated in roots by the salinity and drought stresses, which upregulated the *PgmiR156q*- and *PgmiR529b*-targeted *PgSBP*s. These results support the idea that the expression levels of some of the *PgSBP*s are regulated by *PgmiR156q* and *PgmiR529b*.

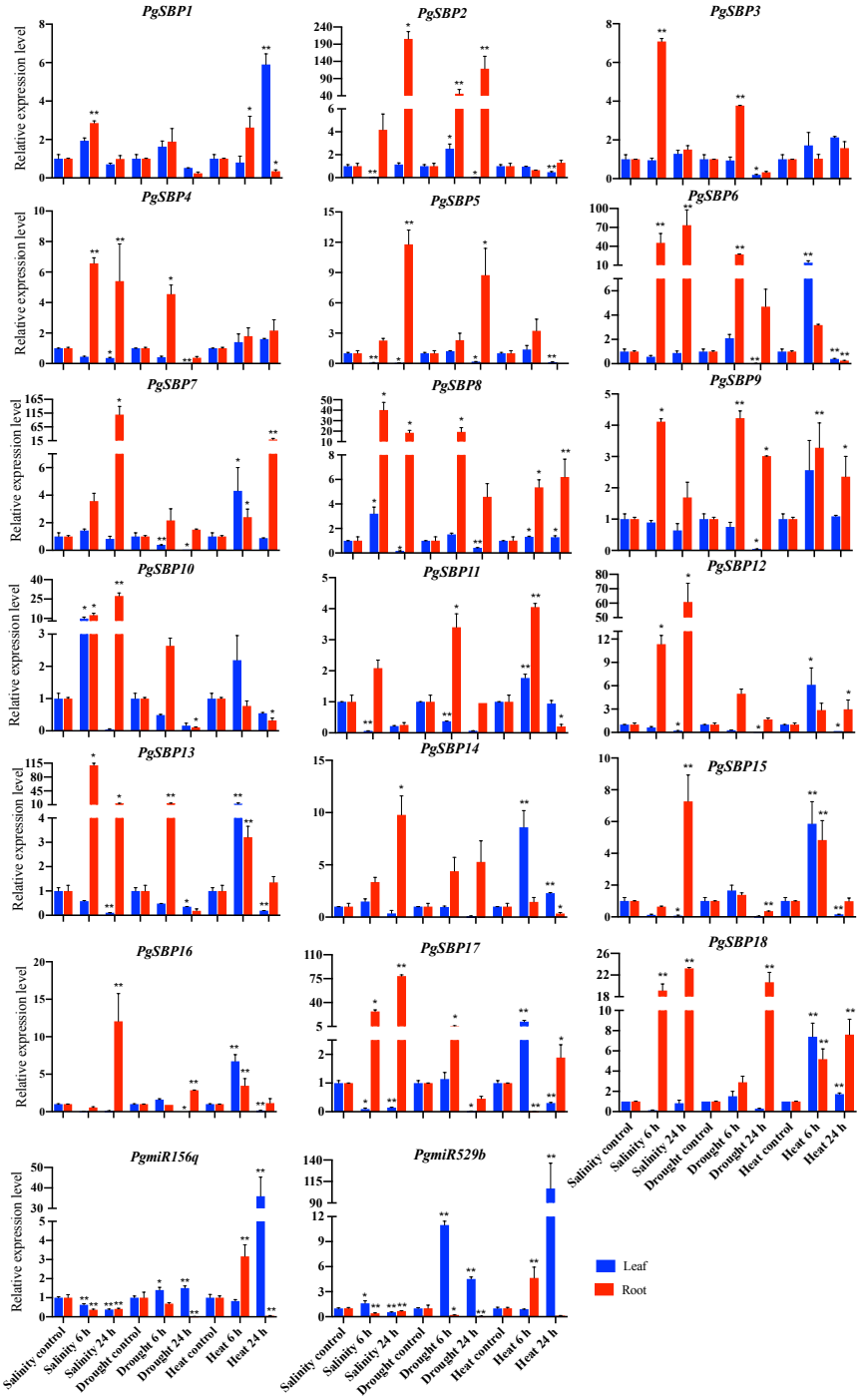

Figure 3.11. The expression levels of *PgSBP*s, *PgmiR156q*, and *PgmiR529b* in leaves and roots in the presence of abiotic stresses. Four-week-old plants were treated with 250 mM NaCl (Salinity), 42°C (Heat), and 15% (W/V) PEG6000 (Drought) for 6 h and 24 h. The expression levels were calculated by the $2^{-\Delta\Delta Ct}$ method. Asterisks indicate significant differences from each control. * $P < 0.05$, **$P < 0.01$, Student's t-test

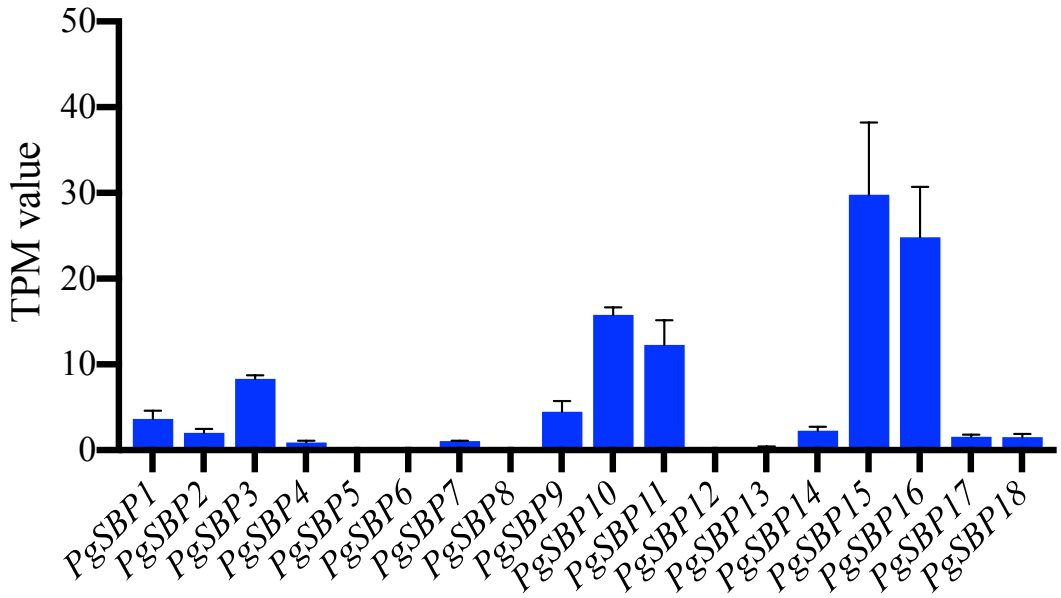

Figure 3.12. The expression levels of *PgSBP*s in root of pearl millet under control condition. The TPM values were retrieved from transcriptome data of previous study.

3.7 Expression profiles of *PgSBP*s, *PgmiR156q*, and *PgmiR529b* in different tissues under ABA treatment

Expression levels of the 18 *PgSBP*s were analyzed in roots and leaves treated with 25 μM ABA (Figure 3.13). All of these *PgSBP*s were downregulated by a 24-h ABA treatment in leaf tissues and many of these genes were also downregulated by the same treatment in root tissues. In contrast, the expression levels of *PgmiR156q* and *PgmiR529b* were increased in both leaves and roots by the ABA treatment. These results suggest that ABA induces *PgmiR156q* and *PgmiR529b*-*PgSBP*s and thereby downregulates *PgSBP*s.

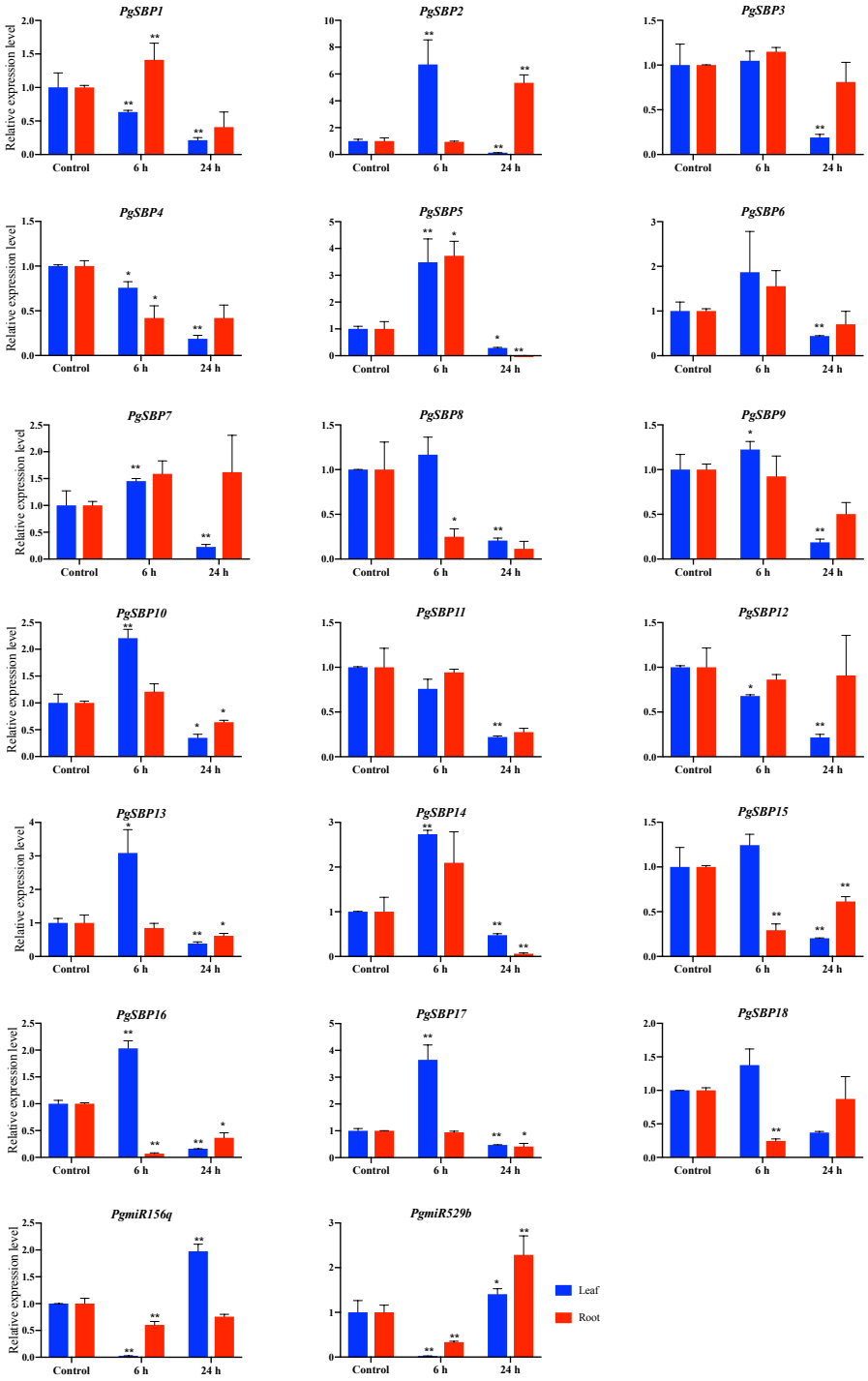

Figure 3.13. The expression level of *PgSBP*s, *PgmiR156q*, and *PgmiR529b* in leaves and roots in the presence of ABA. Four-week-old plants were treated with 25 μM ABA for 6 h and 24 h. The expression levels were calculated by the $2^{-\Delta\Delta Ct}$ method. Asterisks indicate significant differences from each control. * $P < 0.05$, **$P < 0.01$, Student's t-test.

Chapter 4

Discussion

Pearl millet is the sixth most economically important C4 cereal crop with nutrient-rich seeds to provide food security for almost 90 million people inhabiting across the high-temperature regions of Africa and Asia (Shivhare and Lata, 2017). It is a good crop to select stress-responsive genes for breeding stress-tolerant crops, as well as to better understand the stress tolerance mechanisms in plants.

There are a lot of datasets were available for pearl millet, including genome sequence (Varshney et al., 2017), drought stress-responsive (Dudhate et al., 2018) and salinity stress-responsive (Shinde et al., 2018) genes, and salinity stress-responsive microRNAs (Shinde et al., 2020). However, the further analysis of these stress-responsive genes and microRNAs was limited.

Transcription factors (TFs) play vital roles in regulating physiological processes and adapting environmental stresses through various signal transduction pathways (Chen and Rajewsky, 2007). In pearl millet, comprehensive analysis of NAC transcription factor family (Dudhate et al., 2020) and WRKY transcription factors (Chanwala et al., 2020) were performed. *SQUAMOSA* promoter binding protein (SBP) genes encode a plant-specific family of TFs, which play essential roles in plant growth, development, and stress responsiveness. Therefore, it is necessary to do a comprehensive analysis for the SBP family in pearl millet.

In this study, 18 *PgSBP*s were identified in the pearl millet genome (Table 3.1). This number is similar to the numbers of *SBP*-like genes in *Arabidopsis thaliana* (16) (Cardon et al., 1999), *Betula luminifera* (18) (Lin et al., 2018), *Oryza sativa* (19), *Camellia sinensis* (20) (Wang et al., 2018), and *Carica papaya* (14) (Xu et al., 2020). However, the number is smaller than the numbers of SBP-like genes in *Setaria italica*

(27), *Zea mays* (31) (Mao et al., 2016), and *Glycine max* (41) (Tripathi et al., 2017). This may be because the *SBP*s evolved in a species-specific manner.

The 18 PgSBPs were divided into seven groups based on phylogenetic analysis (Figure 3.5). This is consistent with the classification of SBPs of other species, such as cotton (Zhang et al., 2014), rice (Xie, 2006) and maize (Mao et al., 2016). PgSBPs in group IV have the ANK domain, which is predicted to promote protein-protein interaction (Figure 3.4). The ANK domain is also present in 6 SBPs in maize, 3 SBPs in luminifera, and 6 SBPs in cotton (Mao et al., 2016; Lin et al., 2018; Li and Lu, 2014). These findings suggest that the ANK domain is relevant to the functions of these SBPs.

Many of the 19 rice *SBP*s (*OsSPL1-19*, which correspond to *OsSBP1-19*, respectively, in Figure 3.5) have been characterized. *OsSPL3* can be downregulated by *miR156* and *OsSPL3* induces the expression of the *WRKY71* transcription factor gene, thereby negatively regulating cold stress tolerance (Zhou and Tang, 2019). *OsSPL3* and *OsSPL12* are also known as positive regulators of crown root development (Shao et al., 2019). *OsSPL6* represses the expression of an endoplasmic reticulum stress sensor gene, *OsIRE1*, thereby regulating panicle development (Wang et al., 2018). *OsSPL7* can also be downregulated by *miR156* and *OsSPL7* directly regulates the expression of the auxin-related gene *OsGH3.8*, thereby decreasing the tiller number (Dai et al., 2018b). OsSPL8 regulates the development of ligules and auricles in leaves (Lee et al., 2007). *OsSPL9* is a positive regulator of copper transporter genes and can increase copper contents in shoots (Tang et al., 2016). OsSPL10 induces trichome initiation in leaves and glumes and decreases salt tolerance (Lan et al., 2019). *OsSPL13* can also be downregulated by *miR156* and increases cell sizes in the grain hull, thereby increasing grain length and yield (Si et al., 2016). OsSPL14 decreases the tiller number and increases stem strength, lodging resistance, grain number, and grain weight (Jiao et al., 2010; Miura et al., 2010). OsSPL16 promotes cell proliferation in grains, thereby increasing grain width and yield (Wang et al., 2012). *OsSPL14* and *OsSPL16* as well as their close homolog *OsSPL2* are downregulated by *miR156* (Xie et al., 2006) and

miR529 (Yue et al., 2017). *OsSPL18* can also be downregulated by miR156, and OsSPL18 increases panicle length, grain thickness, the grain number yet decreases the tiller number (Yuan et al., 2019). Our data suggest that pearl millet has close homologs of all of these rice SBP genes (Figure 3.5). Physiological functions of SBP genes are also likely to be conserved in pearl millet and rice, but need to be characterized in pear millet in the future.

Some SBP genes in other species play roles in regulating plant responses to abiotic stresses and phytohormones. For instance, overexpression of an *SBP* gene (*VpSBP16*) from a Chinese wild *Vitis* species in Arabidopsis enhances the tolerance to salinity and drought stresses (Hou et al., 2018). Several SBPs in *Betula luminifera* interact with two DELLA proteins and regulate GA responses (Lin et al., 2018). The overexpression of a *B. luminifera SBP*, *BpSPL9*, enhances tolerance to drought and salinity by scavenging reactive oxygen species (ROS) in *B. platyphylla* Suk (Ning et al., 2017). Some of the 14 SBP genes in papaya (*Carica papaya*) are induced at a specific stage in fruit ripening and this process can be controlled by the phytohormone ethylene (Xu et al., 2020). *TaSPL14*, a close *OsSPL14* homolog in wheat (*Triticum aestivum*), does not regulate the tiller number but binds to the promoters of the ethylene-related genes *TaEIL1*, *TaRAP2.11*, and *TaERF1* and increases their expression, thereby regulating plant height, panicle length, the spikelet number, and grain weight (Cao et al., 2021). In this study, ABA-responsive elements and stress-responsive elements were found in most of the *PgSBP* promoters and ABA treatments reduced the expression levels of these genes. In addition, the expression levels of most *PgSBP*s in roots were increased by various abiotic stresses. Therefore, we hypothesize that PgSBPs play essential roles in pearl millet responses to abiotic stresses and phytohormones.

Chapter 5

Conclusion and future plan

In this study, 18 putative *PgSBP*s (*PgSBP1-PgSBP18*) were identified in the genome of pearl millet based on the SBP domain. They were divided into seven groups (I-VII) based on phylogenetic analysis and the members within same group were found to share similar intron/exon structures and motif composition. *PgSBP*s in group V and group VII were found to be targeted by *PgmiR156q* and *PgmiR529b*, with the potential functions of expression level regulation of their targets. The expression pattern of *PgSBP*s under various treatments and the detected stress-responsive and ABA-responsive *cis*-elements raised a hypothesis that *PgSBP*s played important roles in response to abiotic stresses and their stress responsiveness may be involved in ABA signaling pathway.

Based on our comprehensive analysis of *PgSBP*s under various treatment, eight out of 18 *PgSBP*s (*PgSBP2*, *PgSBP3*, *PgSBP7*, *PgSBP10*, *PgSBP11*, *PgSBP13*, *PgSBP15*, and *PgSBP16*) showed significantly induced by various abiotic stresses, including drought, salinity, and drought. Therefore, it is necessary to study their detailed functions in response to abiotic stresses in the future to better understand the mechanisms of plant abiotic stress responses. This study provides vital information for future to select stress-responsive genes.

References

Agarwal, P.K., Agarwal, P., Jain, P., Jha, B., Reddy, M.K., Sopory, S.K., 2008. Constitutive overexpression of a stress-inducible small GTP-binding protein PgRab7 from Pennisetum glaucum enhances abiotic stress tolerance in transgenic tobacco. Plant Cell Rep. 27, 105–115.

Arshad, M., Feyissa, B.A., Amyot, L., Aung, B., Hannoufa, A., 2017. MicroRNA156 improves drought stress tolerance in alfalfa (*Medicago sativa*) by silencing SPL13. Plant Sci. 258, 122–136.

Bailey-Serres, J., Lee, S.C., Brinton, E., 2012. Waterproofing crops: Effective flooding survival strategies. Plant Physiol. 160, 1698–1709.

Bailey, T.L., Boden, M., Buske, F.A., Frith, M., Grant, C.E., Clementi, L., Ren, J., Li, W.W., Noble, W.S., 2009. MEME suite: Tools for motif discovery and searching. Nucleic Acids Res. 37, 202–208.

Boyer, J.S., 1982. Plant productivity and environment. Science 218, 443–448.

Cao, J., Liu, K., Song, W., Zhang, J., Yao, Y., Xin, M., Hu, Z., Peng, H., Ni, Z., Sun, Q., Du, J., 2021. Pleiotropic function of the SQUAMOSA PROMOTER-BINDING PROTEIN-LIKE gene TaSPL14 in wheat plant architecture. Planta 253, 1–12.

Cardon, G., Höhmann, S., Klein, J., Nettesheim, K., Saedler, H., Huijser, P., 1999. Molecular characterisation of the *Arabidopsis* SBP-box genes. Gene 237, 91–104.

Chang, J., Yan, F., Qiao, L., Zheng, J., Zhang, F., Liu, Q., 2016. Genome-wide identification and expression analysis of SBP-box gene family in Sorghum bicolor L. Yi chuan = Hered. 38, 569–580.

Chanwala, J., Satpati, S., Dixit, A., Parida, A., Giri, M.K., Dey, N., 2020. Genome-wide identification and expression analysis of WRKY transcription factors

in pearl millet (*Pennisetum glaucum*) under dehydration and salinity stress. BMC Genomics 21, 231.

Chen, K., Rajewsky, N., 2007. The evolution of gene regulation by transcription factors and microRNAs. Nat. Rev. Genet. 8, 93–103.

Chen, X., 2009. Small RNAs and their roles in plant development. Annu. Rev. Cell Dev. Biol. 25, 21–44.

Crooks, G., Hon, G., Chandonia, J., Brenner, S., 2004. NCBI GenBank FTP Site\nWebLogo: a sequence logo generator. Genome Res 14, 1188–1190.

Cui, L.G., Shan, J.X., Shi, M., Gao, J.P., Lin, H.X., 2014. The miR156-SPL9-DFR pathway coordinates the relationship between development and abiotic stress tolerance in plants. Plant J. 80, 1108–1117.

Cutler, S.R., Rodriguez, P.L., Finkelstein, R.R., Abrams, S.R., 2010. Abscisic acid: emergence of a core signaling network. Annu. Rev. Plant Biol. 61, 651–679.

Dai, X., Zhuang, Z., Zhao, P.X., 2018a. PsRNATarget: A plant small RNA target analysis server (2017 release). Nucleic Acids Res. 46, W49–W54.

Dai, Z., Wang, J., Yang, X., Lu, H., Miao, X., Shi, Z., 2018b. Modulation of plant architecture by the miR156f-OsSPL7-OsGH3.8 pathway in rice. J. Exp. Bot. 69, 5117–5130.

Deng, W., Wang, Y., Liu, Z., Cheng, H., Xue, Y., 2014. HemI: A toolkit for illustrating heatmaps. PLoS One 9, e1119888.

Dudhate, A., Shinde, H., Tsugama, D., Liu, S., Takano, T., 2018. Transcriptomic analysis reveals the differentially expressed genes and pathways involved in drought tolerance in pearl millet [*pennisetum glaucum* (l.) r. Br]. PLoS One 13, 1–14.

Dudhate, A., Shinde, H., Yu, P., Tsugama, D., Gupta, S.K., Liu, S., Takano, T., 2020. Comprehensive analysis of NAC transcription factor family in pearl millet uncovers drought and salinity stress responsive NAC in pearl millet (*Pennisetum Glaucum*) 1–15.

Finkelstein, R., 2013. Abscisic acid synthesis and response. Arab. B. 11, e0166–e0166.

Finkelstein, R., Reeves, W., Ariizumi, T., Steber, C., 2008. Molecular aspects of seed dormancy. Annu. Rev. Plant Biol. 59, 387–415.

Gou, J., Fu, C., Liu, S., Tang, C., Debnath, S., Flanagan, A., Ge, Y., Tang, Y., Jiang, Q., Larson, P.R., Wen, J., Wang, Z.Y., 2017. The miR156-SPL4 module predominantly regulates aerial axillary bud formation and controls shoot architecture. New Phytol. 829–840.

Gou, J.Y., Felippes, F.F., Liu, C.J., Weigel, D., Wang, J.W., 2011. Negative regulation of anthocyanin biosynthesis in Arabidopsis by a miR156-targeted SPL transcription factor. Plant Cell 23, 1512–1522.

H Wani, S., 2015. Plant stress tolerance: Engineering ABA: A potent phytohormone. Transcr. Open Access 03, 1000113.

Harris, J.M., 2015. Abscisic acid: Hidden architect of root system structure. Plants (Basel, Switzerland) 4, 548–572.

Hasanuzzaman, M., Nahar, K., Alam, M.M., Roychowdhury, R., Fujita, M., 2013. Physiological, biochemical, and molecular mechanisms of heat stress tolerance in plants. Int. J. Mol. Sci. 14, 9643-9684.

Hou, H., Jia, H., Yan, Q., Wang, X., 2018. Overexpression of a SBP-box gene (VpSBP16) from chinese wild vitis species in *Arabidopsis* improves salinity and drought stress tolerance. Int. J. Mol. Sci. 19, 940.

Hu, B., Jin, J., Guo, A.Y., Zhang, H., Luo, J., Gao, G., 2015. GSDS 2.0: An upgraded gene feature visualization server. Bioinformatics 31, 1296–1297.

Jiao, Y., Wang, Y., Xue, D., Wang, J., Yan, M., Liu, G., Dong, G., Zeng, D., Lu, Z., Zhu, X., Qian, Q., Li, J., 2010. Regulation of OsSPL14 by OsmiR156 defines ideal plant architecture in rice. Nat. Genet. 42, 541–544.

Kim, T.H., Böhmer, M., Hu, H., Nishimura, N., Schroeder, J.I., 2010. Guard cell signal transduction network: advances in understanding abscisic acid, CO_2, and Ca^{2+} signaling. Annu. Rev. Plant Biol. 61, 561–591.

Klein, J., Saedler, H., Huijser, P., 1996. A new family of DNA binding proteins includes putative transcriptional regulators of the Antirrhinum majus floral meristem identity gene*SQUAMOSA*. Mol. Gen. Genet. MGG. 250, 7–16.

Kumar, S., Hash, C.T., Thirunavukkarasu, N., Singh, G., Rajaram, V., Rathore, A., Senapathy, S., Mahendrakar, M.D., Yadav, R.S., Srivastava, R.K., 2016a. Mapping quantitative trait loci controlling high iron and zinc content in self and open pollinated grains of *Pearl Millet* [*Pennisetum glaucum* (L.) R. Br.]. Front. Plant Sci. 7, 1636.

Kumar, S., Stecher, G., Tamura, K., 2016b. MEGA7: Molecular evolutionary genetics analysisversion 7.0 for bigger datasets. Mol. Biol. Evol. 33, 1870–1874.

Lan, T., Zheng, Y., Su, Z., Yu, S., Song, H., Zheng, X., Lin, G., Wu, W., 2019. OsSPL10, a SBP-Box gene, plays a dual role in salt tolerance and trichome formation in rice (*Oryza sativa* L.). G3 Genes, Genomes, Genet. 9, 4107–4114.

Lee, J., Park, J.J., Kim, S.L., Yim, J., An, G., 2007. Mutations in the rice liguleless gene result in a complete loss of the auricle, ligule, and laminar joint. Plant Mol. Biol. 65, 487–499.

Lescot, M., 2002. PlantCARE, a database of plant cis-acting regulatory elements and a portal to tools for in silico analysis of promoter sequences. Nucleic Acids Res. 30, 325–327.

Letunic, I., Bork, P., 2019. Interactive tree of life (iTOL) v4: recent updates and new developments. Nucleic Acids Res. 47, W256–W259.

Li, C., Lu, S., 2014. Molecular characterization of the SPL gene family in *Populus trichocarpa*. BMC Plant Biol. 14, 131.

Lin, E.P., Niu, M.Y., Huang, H.H., Li, X.Y., Zhang, J.H., Tong, Z.K., 2018. Molecular characterization of SQUAMOSA PROMOTER BINDING PROTEIN-LIKE (SPL) gene family in Betula luminifera. Front. Plant Sci. 9, 1–17.

Mao, H. De, Yu, L.J., Li, Z.J., Yan, Y., Han, R., Liu, H., Ma, M., 2016. Genome-wide analysis of the SPL family transcription factors and their responses to abiotic stresses in maize. Plant Gene 6, 1–12.

Matthews, C., Arshad, M., Hannoufa, A., 2019. Alfalfa response to heat stress is modulated by *microRNA156*. Physiol. Plant. 165, 830–842.

Meena, R.P., Vishwakarma, H., Ghosh, G., Gaikwad, K., Chellapilla, T.S., Singh, M.P., Padaria, J.C., 2020. Novel ASR isolated from drought stress responsive SSH library in pearl millet confers multiple abiotic stress tolerance in PgASR3 transgenic *Arabidopsis*. Plant Physiol. Biochem. 156, 7–19.

Michaely, P., Bennett, V., 1992. The ANK repeat: a ubiquitous motif involved in macromolecular recognition. Trends Cell Biol. 2, 127–129.

Miura, K., Ikeda, M., Matsubara, A., Song, X.J., Ito, M., Asano, K., Matsuoka, M., Kitano, H., Ashikari, M., 2010. OsSPL14 promotes panicle branching and higher grain productivity in rice. Nat. Genet. 42, 545–549.

Nambiar, V.S., Dhaduk, J.J., Sareen, N., Shahu, T., Desai, R., 2011. Potential functional implications of pearl millet (*Pennisetum glaucum*) in health and disease. J. Appl. Pharm. Sci. 1, 62–67.

Ning, K., Chen, S., Huang, H., Jiang, J., Yuan, H., Li, H., 2017. Molecular characterization and expression analysis of the SPL gene family with *BpSPL9* transgenic lines found to confer tolerance to abiotic stress in Betula platyphylla Suk. Plant Cell, Tissue Organ Cult. 130, 469–481.

Qin, F., Shinozaki, K., Yamaguchi-Shinozaki, K., 2011. Achievements and challenges in understanding plant abiotic stress responses and tolerance. Plant Cell Physiol. 52, 1569–1582.

Rajagopal, D., Agarwal, P., Tyagi, W., Singla-Pareek, S.L., Reddy, M.K., Sopory, S.K., 2007. Pennisetum glaucum Na^+/H^+ antiporter confers high level of salinity tolerance in transgenic Brassica juncea. Mol. Breed. 19, 137–151.

Reddy, P.S., Mallikarjuna, G., Kaul, T., Chakradhar, T., Mishra, R.N., Sopory, S.K., Reddy, M.K., 2010. Molecular cloning and characterization of gene encoding for cytoplasmic Hsc70 from Pennisetum glaucum may play a protective role against abiotic stresses. Mol. Genet. Genomics 283, 243–254.

Schmittgen, T.D., Livak, K.J., 2008. Analyzing real-time PCR data by the comparative CT method. Nat. Protoc. 3, 1101–1108.

Seki, M., Ishida, J., Narusaka, M., Fujita, M., Nanjo, T., Umezawa, T., Kamiya, A., Nakajima, M., Enju, A., Sakurai, T., Satou, M., Akiyama, K., Yamaguchi-Shinozaki, K., Carninci, P., Kawai, J., Hayashizaki, Y., Shinozaki, K., 2002. Monitoring the expression pattern of around 7,000 Arabidopsis genes under ABA treatments using a full-length cDNA microarray. Funct. Integr. Genomics 2, 282–291.

Shao, Y., Zhou, H.Z., Wu, Y., Zhang, H., Lin, J., Jiang, X., He, Q., Zhu, J., Li, Y., Yu, H., Mao, C., 2019. OsSPL3, an SBP-domain protein, regulates crown root development in rice. Plant Cell 31, 1257-1275.

Shinde, H., Dudhate, A., Anand, L., Tsugama, D., Gupta, S.K., Liu, S., Takano, T., 2020. Small RNA sequencing reveals the role of pearl millet miRNAs and their targets in salinity stress responses. South African J. Bot. 132, 395–402.

Shinde, H., Dudhate, A., Tsugama, D., Gupta, S.K., Liu, S., Takano, T., 2019. Pearl millet stress-responsive NAC transcription factor *PgNAC21* enhances salinity stress tolerance in Arabidopsis. Plant Physiol. Biochem. 135, 546–553.

Shinde, H., Tanaka, K., Dudhate, A., Tsugama, D., Mine, Y., Kamiya, T., K. Gupta, S., Liu, S., Takano, T., 2018. Comparative de novo transcriptomic profiling of the salinity stress responsiveness in contrasting pearl millet lines. Environ. Exp. Bot. 155, 619–627.

Shinozaki, K., Yamaguchi-Shinozaki, K., 2007. Gene networks involved in drought stress response and tolerance. J. Exp. Bot. 58, 221–227.

Shivhare, R., Lata, C., 2017. Exploration of genetic and genomic resources for abiotic and biotic stress tolerance in pearl millet. Front. Plant Sci. 7, 1–17.

Si, L., Chen, J., Huang, X., Gong, H., Luo, J., Hou, Q., Zhou, T., Lu, T., Zhu, J., Shangguan, Y., Chen, E., Gong, C., Zhao, Q., Jing, Y., Zhao, Y., Li, Y., Cui, L., Fan, D., Lu, Y., Weng, Q., Wang, Y., Zhang, Q., Liu, K., Wei, X., An, K., An, G., Han, B., 2016. OsSPL13 controls grain size in cultivated rice. Nature Genetics 48, 447–456.

Sreenivasulu, N., Harshavardhan, V.T., Govind, G., Seiler, C., Kohli, A., 2012. Contrapuntal role of ABA: does it mediate stress tolerance or plant growth retardation under long-term drought stress? Gene 506, 265–273.

Tang, M., Zhou, C., Meng, L., Mao, D., Peng, C., Zhu, Y., Huang, D., Tan, Z., Chen, C., Liu, C., Zhang, D., 2016. Overexpression of OsSPL9 enhances accumulation of Cu in rice grain and improves its digestibility and metabolism. J. Genet. Genomics 43, 673–676.

Tilman, D., Balzer, C., Hill, J., Befort, B.L., 2011. Global food demand and the sustainable intensification of agriculture. Proc. Natl. Acad. Sci. 108, 20260–20264.

Tripathi, R.K., Goel, R., Kumari, S., Dahuja, A., 2017. Genomic organization, phylogenetic comparison, and expression profiles of the SPL family genes and their regulation in soybean. Dev. Genes Evol. 227, 101–119.

Vadez, V., Hash, T., Bidinger, F., Kholova, J., 2012. Phenotyping pearl millet for adaptation to drought. Front. Physiol. 3, 386.

Varshney, R.K., Shi, C., Thudi, M., Mariac, C., Wallace, J., Qi, P., Zhang, H., Zhao, Y., Wang, X., Rathore, A., Srivastava, R.K., Chitikineni, A., Fan, G., Bajaj, P., Punnuri, S., Gupta, S.K., Wang, H., Jiang, Y., Couderc, M., Katta, M.A.V.S.K., Paudel, D.R., Mungra, K.D., Chen, W., Harris-Shultz, K.R., Garg, V., Desai, N., Doddamani, D., Kane, N.A., Conner, J.A., Ghatak, A., Chaturvedi, P., Subramaniam,

S., Yadav, O.P., Berthouly-Salazar, C., Hamidou, F., Wang, Jianping, Liang, X., Clotault, J., Upadhyaya, H.D., Cubry, P., Rhoné, B., Gueye, M.C., Sunkar, R., Dupuy, C., Sparvoli, F., Cheng, S., Mahala, R.S., Singh, B., Yadav, R.S., Lyons, E., Datta, S.K., Hash, C.T., Devos, K.M., Buckler, E., Bennetzen, J.L., Paterson, A.H., Ozias-Akins, P., Grando, S., Wang, Jun, Mohapatra, T., Weckwerth, W., Reif, J.C., Liu, X., Vigouroux, Y., Xu, X., 2017. Pearl millet genome sequence provides a resource to improve agronomic traits in arid environments. Nat. Biotechnol. 35, 969–976.

Wang, J.W., Czech, B., Weigel, D., 2009. miR156-regulated SPL transcription factors define an endogenous flowering pathway in Arabidopsis thaliana. Cell 138, 738–749.

Wang, P., Chen, D., Zheng, Y., Jin, S., Yang, J., Ye, N., 2018. Identification and expression analyses of SBP-box genes reveal their involvement in abiotic stress and hormone response in tea plant (Camellia sinensis). Int. J. Mol. Sci. 19, 3404.

Wang, S., Wu, K., Yuan, Q., Liu, X., Liu, Z., Lin, X., Zeng, R., Zhu, H., Dong, G., Qian, Q., Zhang, G., Fu, X., 2012. Control of grain size, shape and quality by OsSPL16 in rice. Nat. Genet. 44, 950–954.

Wang, W., Vinocur, B., Altman, A., 2003. Plant responses to drought, salinity and extreme temperatures: towards genetic engineering for stress tolerance. Planta 218, 1–14.

Xie, K., Wu, C., Xiong, L., 2006. Genomic organization, differential expression, and interaction of SQUAMOSA promoter-binding-like transcription factors and microRNA156 in rice. Plant Physiol. 142, 280–293.

Xiong, L., Yang, Y., 2003. Disease resistance and abiotic stress tolerance in rice are inversely modulated by an abscisic acid–inducible mitogen-activated protein kinase. Plant Cell 15, 745–759.

Xu, Y., Xu, H., Wall, M.M., Yang, J., 2020. Roles of transcription factor SQUAMOSA promoter binding protein-like gene family in papaya (Carica papaya) development and ripening. Genomics 112, 2734–2747.

Yamaguchi-Shinozaki, K., Shinozaki, K., 2006. Transcriptional regulatory networks in cellular responses and tolerance to dehydration and cold stresses. Annu. Rev. Plant Biol. 57, 781–803.

Yamasaki, K., Kigawa, T., Inoue, M., Tateno, M., Yamasaki, T., Yabuki, T., Aoki, M., Seki, E., Matsuda, T., Nunokawa, E., Ishizuka, Y., Terada, T., Shirouzu, M., Osanai, T., Tanaka, A., Seki, M., Shinozaki, K., Yokoyama, S., 2004. A novel zinc-binding motif revealed by solution structures of DNA-binding domains of Arabidopsis SBP-family transcription factors. J. Mol. Biol. 337, 49–63.

Yu, N., Niu, Q.W., Ng, K.H., Chua, N.H., 2015. The role of miR156/SPLs modules in Arabidopsis lateral root development. Plant J. 83, 673–685.

Yu, S., Galvão, V.C., Zhang, Y.C., Horrer, D., Zhang, T.Q., Hao, Y.H., Feng, Y.Q., Wang, S., Schmid, M., Wang, J.W., 2012. Gibberellin regulates the Arabidopsis floral transition through miR156-targeted SQUAMOSA PROMOTER BINDING–LIKE transcription factors . Plant Cell 24, 3320–3332.

Yuan, H., Qin, P., Hu, L., Zhan, S., Wang, S., Gao, P., Li, J., Jin, M., Xu, Z., Gao, Q., Du, A., Tu, B., Chen, W., Ma, B., Wang, Y., Li, S., 2019. *OsSPL18* controls grain weight and grain number in rice. J. Genet. Genomics 46, 41–51.

Yue, E., Li, C., Li, Y., Liu, Z., Xu, J.H., 2017. *MiR529a* modulates panicle architecture through regulating SQUAMOSA PROMOTER BINDING-LIKE genes in rice (Oryza sativa). Plant Mol. Biol. 94, 469–480.

Zhang, H.X., Jin, J.H., He, Y.M., Lu, B.Y., Li, D.W., Chai, W.G., Khan, A., Gong, Z.H., 2016. Genome-wide identification and analysis of the SBP-box family genes under phytophthora capsici stress in Pepper (Capsicum annuum L.). Front. Plant Sci. 7, 1–14.

Zhang, S.D., Ling, L.Z., 2018. Diversification of *SQUANOSA* promoter binding protein-like (SPL) genes by changes of miR156/529 binding sites in land plants. Plant Gene 14, 55–63.

Zhang, X., Dou, L., Pang, C., Song, M., Wei, H., Fan, S., Wang, C., Yu, S., 2014. Genomic organization, differential expression, and functional analysis of the SPL gene family in Gossypium hirsutum. Mol. Genet. Genomics 290, 115–126.

Zhou, M., Tang, W., 2019. MicroRNA156 amplifies transcription factor-associated cold stress tolerance in plant cells. Mol. Genet. Genomics 294, 379–393.

Acknowledgements

Upon the coming of my graduate time, I would like to express heartfelt thanks to all those who have offered me assistance and support during the four years of my doctoral course in the Department of Agricultural and Environmental Biology and Asian Research Center for Bioresource and Environmental Sciences (ARC-BRES), Graduate School of Agricultural and Life Sciences, the University of Tokyo.

Firstly, I would like to express my deepest appreciation to my supervisor, Prof. Dr. Tetsuo Takano, for his creative guidance, all suggestions, and constant encouragement throughout my doctor course. I feel deeply thankful and fortunate to be a student in his laboratory.

I also want to extant my thanks to Associate Prof. Dr. Daisuke Tsugama, for his precious suggestions and patient guidance in my research work. Besides, I would like to express my sincere gratitude to Prof. Dr. Chunlan Lian, who gave me irreplaceable helps during my daily life. I also express my gratitude to Prof. Dr. Shenkui Liu of Zhejiang A&F University, who guided my research to the correct direction. I would like to thank Dr. Shashi Kumar Gupta of International Crops Research Institute for the Semi-Arid Tropics (ICRISAT), India, for providing the pearl millet seeds.

I would like to thank my seniors Dr. Harshraj Shinde and Dr. Ambika Dudhate, who taught many experimental skills and experiences in my research work and daily life. I also want to extend my deep thanks to all members of Takano and Tsugama laboratory for their kind help and support in the four years.

Finally, I would like to give my deep gratefulness and love to my family and my friends, especially to my husband Dr. Zhenxing Xu and my lovely son, Yikang Xu, whose accompany and support really encouraged me to complete my doctoral course. They are my forever harbor in my life.